

Article

Genomic and Experimental Investigations of *Auriscalpium* and *Strobilurus* Fungi Reveal New Insights into Pinecone Decomposition

Panmeng Wang^{1,2,3}, Jianping Xu⁴ , Gang Wu^{1,2}, Tiezhi Liu⁵ and Zhu L. Yang^{1,2,*}

- ¹ CAS Key Laboratory for Plant Diversity and Biogeography of East Asia, Kunming Institute of Botany, Chinese Academy of Sciences, Kunming 650201, China; wangpanmeng@mail.kib.ac.cn (P.W.); wugang@mail.kib.ac.cn (G.W.)
- ² Yunnan Key Laboratory for Fungal Diversity and Green Development, Kunming Institute of Botany, Chinese Academy of Sciences, Kunming 650201, China
- ³ University of Chinese Academy of Sciences, Beijing 100049, China
- ⁴ Department of Biology, McMaster University, Hamilton, ON L8S 4K1, Canada; jpxu@mcmaster.ca
- ⁵ College of Life Sciences, Chifeng University, Chifeng 024000, China; tiezhiliu@aliyun.com
- * Correspondence: fungi@mail.kib.ac.cn

Abstract: Saprophytic fungi (SPF) play vital roles in ecosystem dynamics and decomposition. However, because of the complexity of living systems, our understanding of how SPF interact with each other to decompose organic matter is very limited. Here we studied their roles and interactions in the decomposition of highly specialized substrates between the two genera *Auriscalpium* and *Strobilurus* fungi-colonized fallen pinecones of the same plant sequentially. We obtained the genome sequences from seven fungal species with three pairs: *A. orientale*-*S. luchuensis*, *A. vulgare*-*S. stephanocystis* and *A. microsporium*-*S. pachycystidiatus*/*S. orientalis* on cones of *Pinus yunnanensis*, *P. sylvestris* and *P. armandii*, respectively, and the organic profiles of substrate during decomposition. Our analyses revealed evidence for both competition and cooperation between the two groups of fungi during decomposition, enabling efficient utilization of substrates with complementary profiles of carbohydrate active enzymes (CAZymes). The *Auriscalpium* fungi are highly effective at utilizing the primary organic carbon, such as lignin, and hemicellulose in freshly fallen cones, facilitated the invasion and colonization by *Strobilurus* fungi. The *Strobilurus* fungi have genes coding for abundant CAZymes to utilize the remaining organic compounds and for producing an arsenal of secondary metabolites such as strobilurins that can inhibit other fungi from colonizing the pinecones.

Keywords: successive decomposition; *Auriscalpium*; *Strobilurus*; carbohydrate active enzymes; competition; secondary metabolites; strobilurin



Citation: Wang, P.; Xu, J.; Wu, G.; Liu, T.; Yang, Z.L. Genomic and Experimental Investigations of *Auriscalpium* and *Strobilurus* Fungi Reveal New Insights into Pinecone Decomposition. *J. Fungi* **2021**, *7*, 679. <https://doi.org/10.3390/jof7080679>

Academic Editor: Raffaella Maria Balestrini

Received: 13 July 2021

Accepted: 19 August 2021

Published: 23 August 2021

Publisher's Note: MDPI stays neutral with regard to jurisdictional claims in published maps and institutional affiliations.



Copyright: © 2021 by the authors. Licensee MDPI, Basel, Switzerland. This article is an open access article distributed under the terms and conditions of the Creative Commons Attribution (CC BY) license (<https://creativecommons.org/licenses/by/4.0/>).

1. Introduction

Decomposition of organic matter is vitally important in ecosystem processes such as carbon and nitrogen cycling, soil formation and biodiversity maintenance [1,2]. In nature, decomposition is highly dynamic with ever-changing interactions among decomposers and between substrate composition and successive development of microbial communities [3,4]. Fungi are key components of the microbial communities in most natural decompositions with different fungal species interacting with each other in multiple ways, leading to complete degradation of complex organic compounds such as lignocelluloses in wood and plant litter. Indeed, there is emerging evidence showing orderly succession among fungal members of microbial communities through the different stages of lignocellulose decomposition [5].

As one of the most important members of microbial communities in forest ecosystems, saprotrophic fungi (SPF) have diverse degradation mechanisms and play key roles in the degradations of dead organic matters [3,6]. However, due to the limited resources across

space and time in most ecological niches and the presence of many (potential) competitors, fungal decomposers have evolved mechanisms to allow them successfully colonizing one to several substrates/ecological niches [7]. Those colonizing only one type of ecological niche are called ecological “specialists” while others capable of colonizing many types of ecological niches are called “generalists” [8]. There are many who are in-between the obligate specialists and broad generalists, including those that are primarily found in one ecological niche but are capable of surviving and growing in other niches [8]. Evidence for ecological specializations in fungi has been recorded since ancient times [3]. In addition, most ecological niches and substrates have successions where different fungal communities may dominate different phases of substrate decomposition [5].

There are many factors that can impact the composition and structure of saprotrophic fungal community. Among these factors, the chemical composition of substrates plays a major role [9,10]. For example, on woody substrates, the decomposition rate of polymeric lignocellulosic components changes through the decomposition process, due to changes in substrate compositions and in the types and relative abundances of different microbes and their enzymes involved in degradations [11]. Traditionally, saprotrophic fungi are broadly classified into two types, namely ligninolytic white-rot (WR) and cellulolytic brown-rot (BR), although there is a continuum between these two types [7,12]. In the process of decomposition, interaction (including competition) among fungi is likely very common, affecting the distribution, abundance, and the order of occurrence among these fungi in natural communities [13].

Different interaction strategies among species can lead to different orders of SPF colonization on substrates. Both biotic and abiotic factors can also influence their order of colonization and interactions [7,14,15]. Fungal competition on substrates is commonly classified into two major functional types: primary resource capture and secondary resource capture [7,16,17]. Success of SPF in primary resource capture mainly depends on the ability to utilize previously uncolonized resources and on their ability to resist plant derived antifungal compounds in those substrates. In contrast, success in secondary resource capture mainly relies on antagonistic mechanisms (i.e., antifungal production etc.), with different species competing with each other to obtain sufficient nutrients for survival and reproduction [7]. Often, changes in microbial communities during decomposition are related to the secretion of antagonistic enzymes and metabolites [7]. On the one hand, SPFs have the ability to secrete various carbohydrate-active enzymes (CAZymes) to decompose and utilize the major constituents such as lignin, cellulose and hemicellulose in wood and plant litter, facilitating nutrient cycling and energy flow in forest ecosystem [18–20]. Indeed, the compositions and characteristics of CAZymes often differ among fungi, likely shaped by characteristics of their substrates and the degree of adaptation to the specific environmental conditions [20]. Therefore, to understand decomposition, it is particularly important to study the compositions and characteristics of CAZymes to clarify the potential mechanisms for different nutritional modes, infection and substrates specificity/preference [20–25]. On the other hand, fungal secondary metabolites (SMs) are known to play crucial roles in the defense against pathogens and competitors and provide advantages for their producers and/or those who have resistant mechanisms. Along with CAZymes, fungal SMs can provide important information for understanding the chemical basis of niche specialization during decompositions [26,27].

Multiple groups of SPFs are frequently involved in plant litter decomposition. These fungi belong to diverse clades, but some of them are functionally interchangeable [26,28,29], Figure S1. In forest ecosystems, due to its extractive composition and the presence of anti-fungal compounds such as resin, pinecone is a specialized substrate and a unique habitat for fungi [30,31]. Indeed, only species in a few fungal genera (e.g., *Strobilurus*, *Auriscalpium*, *Baeospora* and *Mycena*) are known to colonize and decompose pinecones. Among these genera, *Auriscalpium* and *Strobilurus* are highly specialized on pinecones [30,31]. Interestingly, species of *Auriscalpium* and *Strobilurus* usually share the dead cones of the same plant species in a chronological order, with fruiting bodies of *Auriscalpium* fungi often appearing

on newly fallen cones, while those of *Strobilurus* typically occurring on highly rotten cones during later stages of decomposition (Figures S2 and S3). At present, the mechanisms for their succession during pinecone decomposition are unknown.

In this study, we investigated three pinecone substrate–fungus pairs from Europe and East Asia to understand the potential mechanisms for substrate specificities and ecological succession during pinecone decomposition. The three fungal pairs as well as their substrates were *A. orientale*-*S. luchuensis* on cones of *Pinus yunnanensis*, *A. vulgare*-*S. stephanocystis* on cones of *P. sylvestris*, and *A. microsporum*-*S. pachycystidiatus*/*S. orientalis* on cones of *P. armandii*. We obtained the genome sequences of these seven fungal species and quantified the main chemical compounds during pinecone decomposition. Our analyses revealed both shared and unique features in their substrate specificity and ecological successions among these fungal pairs.

2. Materials and Methods

2.1. Material Collections, Greenhouse Planting Experiment, Fungal Strains, Media and Culture Conditions

The records on the geographical distributions and substrate information of *A. vulgare* and *S. stephanocystis* were extracted from data deposited in the Global Biodiversity Information Facility (GBIF; <https://www.gbif.org/>; accessed on 11 April 2019). The information on substrates and distributions of the following four species *A. orientale*, *A. microsporum*, *S. luchuensis* and *S. pachycystidiatus* was primarily from the published literature and our own observations during field investigations in China. In order to directly observe the characteristics of pinecone decomposition by *Auriscalpium* and *Strobilurus*, a planting experiment was conducted in the greenhouse using about 250 cones of *P. armandii* fully colonized by *A. microsporum* collected in Yufeng Temple (Lijiang City, Yunnan Province, China) in July 2017 where both *Auriscalpium* and *Strobilurus* existed. The reason for the selection of collection site of Yufeng Temple is that Yufeng Temple is the distribution center of fungi in *Strobilurus* and *Auriscalpium*, and the climate in this area is close to Kunming City. After we brought cones back without any specific treatment, we put them in the plastic shed and spray water regularly to ensure their humidity. During our experiment, we keep the temperature in the greenhouse consistent with the outdoor temperature of Kunming.

All seven strains used for de novo sequencing were dikaryotic strains isolated directly from the fruiting bodies from wild mushrooms. Among these, the following five species and strains were collected in Yunnan Province, China: *A. microsporum* (strain AU-H-210), *A. orientale* (strain AU-Y-A), *S. luchuensis* (strain Y-Y-2D), *S. pachycystidiatus* (strain Y-H-6C) and *S. orientalis* (strain K-1-1). The remaining two *A. vulgare* (CBS 236.39) and *S. stephanocystis* (CBS 113577) were obtained from the Westerdijk Fungal Biodiversity Institute (CBS, Fungal Biodiversity Centre in Netherlands). The strains were stored at 4 °C on MEA solid medium (1% malt extract, 0.1% peptone and 1.5% agar). Vegetative mycelia of those strains were cultivated in MEA liquid medium (1% malt extract and 0.1% peptone) in the dark at 23 °C for 7–25 days, and then the mycelia were collected for DNA extraction and whole genome sequencing [32].

2.2. Measurements of Pinecone Compositions

For each type of pinecone, we analyzed the complex organic compounds at two different states: (i) newly fallen cones, and (ii) cones being decomposed by fungi in the genus *Auriscalpium* and just colonized by fungi in *Strobilurus* (Figure S3). The contents of cellulose, hemicellulose and lignin were quantified using the automatic fiber analyzer according to the ANKOM 2000i instructions (<https://www.ankom.com/technical-support/fiber-analyzer-a2000>; accessed on 21 April 2019) in cones of *P. armandii*, *P. yunnanensis* and *P. sylvestris* at KIB (Kunming Institute of Botany, CAS) as references. The pectin contents in these samples were quantified by using the method of sulfuric acid-carbazole colorimetry [33]. Analyses for all samples were carried in decuplicate.

2.3. Genome Sequencing, Assembly and Protein-Coding Gene Predictions

To yield a high-quality genome assembly, the genomes were sequenced using a whole genome shotgun sequencing strategy with a combined strategy that included both the Pacific Biosciences RS II (Pacific Biosciences, Menlo Park, CA, USA) and Illumina MiSeq platforms (Illumina Inc., San Diego, CA, USA) by Biomarker Technologies Co, LTD (Beijing, China). The PacBio long reads were corrected and assembled using Canu for draft genomes [34]. FinisherSC was used to improve the contiguity of draft genomes [35], and Pilon was used to polish the draft genomes with collected Illumina data by Musket [36,37]. HaploMerger2 was used to separate the two haploid sub-assemblies from the assembly [38,39]. Ab initio predictions were carried out using the reference protein domains of *Peniophora* sp. and *Armillaria ostoyae* [40,41] for *Auriscalpium* and *Strobilurus*, respectively. Based on the two high-quality sequencing datasets described above, the protein-coding gene set of genomes were refined following the GETA gene annotation method [42]. BUSCOs using database of fungi_odb9 were applied to our gene predictions.

2.4. Identification of Carbohydrate-Active Enzymes (CAZymes) and Lignocellulolytic Genes and Swiss-Prot Annotation

Carbohydrate-active enzymes (CAZymes) were identified by using a combination of pipelines that included the HMM and BLASTP algorithms [43]. CAZyme annotation by BLASTP algorithms used a cutoff *e-value* $< 1 \times 10^{-5}$ and coverage $> 20\%$. CAZyme annotation by HMM algorithms used a cutoff *e-value* $< 1 \times 10^{-5}$ for alignments of > 80 amino acids, and for alignments of < 80 amino acids, we used an *e-value* of $< 1 \times 10^{-3}$ and coverage $> 25\%$. Perl program was used to extract the annotation results that conform to the two methods as the final result. For Swiss-Prot annotation, the BLASTP algorithm was used to align the protein sequences to Swiss-Prot with *e-value* $< 1 \times 10^{-5}$ and coverage $> 20\%$. Lignocellulolytic genes (cellulase, hemicellulase, pectinase, lignin oxidase and lignin degrading auxiliary enzymes) were identified mainly by the Swiss-Prot annotation with keywords as described by Chen et al. [43] in their Table S20. In the following analyses, lignin oxidases and lignin degrading auxiliary enzymes encoded by lignocellulolytic genes were combined into one category called ligninases [43].

2.5. Principal Component Analyses (PCA) and Heatmap Analyses of CAZymes and Lignocellulolytic Genes

In PCA of CAZymes, organisms are clustered with others which have the similar nutrient patterns to determine the rot patterns of fungi. Here, PCA was used to cluster WR and BR fungi based on the diversity of their CAZymes. The CAZymes number matrix of wood decay fungi (WDF) from the following species was used as input: *Galerina marginata* (abbreviated as "gama"), *A. orientale* ("auor"), *Heterobasidion annosum* ("hean"), *Stereum hirsutum* ("sthi"), *A. vulgare* ("auvu"), *Punctularia strigosozonata* ("pust"), *A. microsporum* ("aumi"), *Fomitiporia mediterranea* ("fome"), *S. pachycystidiatus* ("stpa"), *S. luchuensis* ("stlu"), *Dichomitus squalens* ("disq"), *Trametes versicolor* ("trve"), *Phanerochaete chrysosporium* ("phch"), *S. stephanocystis* ("stst"), *Phanerochaete carnosa* ("phca"), *S. orientalis* ("stor"), *Wolfiporia cocos* ("woco"), *Gloeophyllum trabeum* ("gltr"), *Fomitopsis pinicola* ("fopi"), *Dacryopinax primogenitus* ("dapr"), *Serpula lacrymans* ("sela") and *Coniophora puteana* ("copu") [12,44–49].

Among these species, phca, phch, hean, sthi, gama, disq, trve, fome and pust belonged to WR fungi, while copu, gltr, fopi, woco, dapr and sela belonged to BR fungi [12,43]. The online OmicShare tools (<http://www.omicshare.com/tools>; accessed on 14 August 2019) were used to generate the illustrations, heatmaps and other outputs from PCA and statistical analysis. Adobe Photoshop (PS) and Adobe Illustrator (AI) were used for image editing and finalization.

2.6. Analyses of Enzymes on Resin Decomposition

By adding latex to media, Oghenekaro et al. (2020) identified that some genes had elevated expressions in *R. microporus*. Latex is a complex emulsion that includes a diversity

of chemicals such as proteins, alkaloids, carbohydrates, oils, tannins, and resins that coagulate on exposure to air [50,51]. It is commonly produced by plants after tissue injury and serve as a defense against pathogens and pests [50,51]. Here we used the high expressed genes induced by latex treatment in *R. microporus* to infer the distributions of these genes in the seven fungi analyzed in our study. Using those genes in *R. microporus* as references, we identified the homologous genes in our genomes through BLASTP algorithms with a cut off *e-value* $< 1 \times 10^{-5}$ and coverage $>20\%$.

2.7. Secondary Metabolites (SMs) in *Auriscalpium* and *Strobilurus*

SMs genes are frequently located in gene clusters of microorganisms [52], and they may have important physiological and ecological significances with antifungal, antibacterial, antitumor, antiviral, antialgal, immune-suppressive and other biological effects [53]. Here, for our seven genomes, SM gene clusters were determined using a web-based analysis platform named AntiSMASH fungal 6.0 (<https://fungismash.secondarymetabolites.org/#!/start>; accessed on 13 August 2019) [54].

2.8. Species Tree Construction, Divergence Time Estimation and Gene Family Expansions of CAZymes Analysis

Orthologous genes and single-copy orthologous genes among 22 publicly available fungal genomes above were identified by using software of OrthoMCL [55,56] with same parameters of Chen et al. [43]. The generated proteomes and corresponding coding sequences were used as input to phylogenomic and comparative genomic analyses. We constructed a phylogenomic tree included genomes with predicted proteome clusters generated from the comparative analysis of 22 available fungal genomes, with *Dacryopinax primogenitus* as the outgroup. Phylogenomics analysis was conducted based on the framework proposed by Chen et al. [43] using software of ProtTest [57], MAFFT v7.158b [58], Gblocks 0.91b and RAxML-8.0.26 [59]. For divergence time estimation with r8s v1.80 [60] with same parameters of Chen et al. [43], one fossil calibration points and three secondary calibration point [45] were fixed in the molecule clock analysis: the most recent common ancestor (MRCA) of *Serpula lacrymans* and *Coniophora puteana* were diverged at 104.23 million years ago (MYA); the MRCA of *Punctularia strigosozonata* and *Gloeophyllum trabeum* were diverged at 170.42 MYA; the MRCA of *Stereum hirsutum* and *Heterobasidion annosum* were diverged at 100.94 MYA and the MRCA of *Fomitiporia mediterranea* and *Dacryopinax primogenitus* were diverged at 349.72 MYA. The orthologous gene family expansions and contractions were calculated by CAFE with p-values less than 0.05 based on the ultrametric tree [61]. When we got the expanded gene families, we selected the expanded gene families belonging to CAZymes for subsequent analysis.

3. Results

3.1. Ecological Characteristics of Fungi in *Auriscalpium* and *Strobilurus*

The temporal and trophic niches as reported in the literature and our own observations for *Auriscalpium* and *Strobilurus* fungi in this study are summarized in Figures 1, S2 and S3 and Table S1. The data showed clear differences between these two groups of fungi in their temporal distributions during pinecone decomposition (Figures 1, S2 and S3; Table S1). Specifically, fruiting bodies of *A. vulgare* are mostly found on newly fallen cones of *P. sylvestris*, *P. pinaster*, *P. halepensis* and *P. mugo* in September and October, while those of *S. stephanocystis* mostly appear on highly rotten cones already decomposed by *A. vulgare* in May. Similarly, *A. orientale* mainly appears on newly fallen cones of *P. yunnanensis*, *P. tabuliformis*, *P. densiflora*, *P. densata*, *P. massoniana* and *P. hwangshanensis* in August, while *S. luchuensis* on highly rotten cones already decomposed by *A. orientale*. In addition, *A. microsporum* mostly produces fruiting bodies in September on newly fallen cones of *P. armandii* and with fruiting bodies of *S. pachycystidiatus* found in June on cones newly decomposed by *A. microsporum*, and *S. orientalis* in October on highly decomposed cones by *A. microsporum* and/or *S. pachycystidiatus*. Although the time of fruiting was different,

the preferences of the two genera for the substrates with different degrees of decay were not affected.

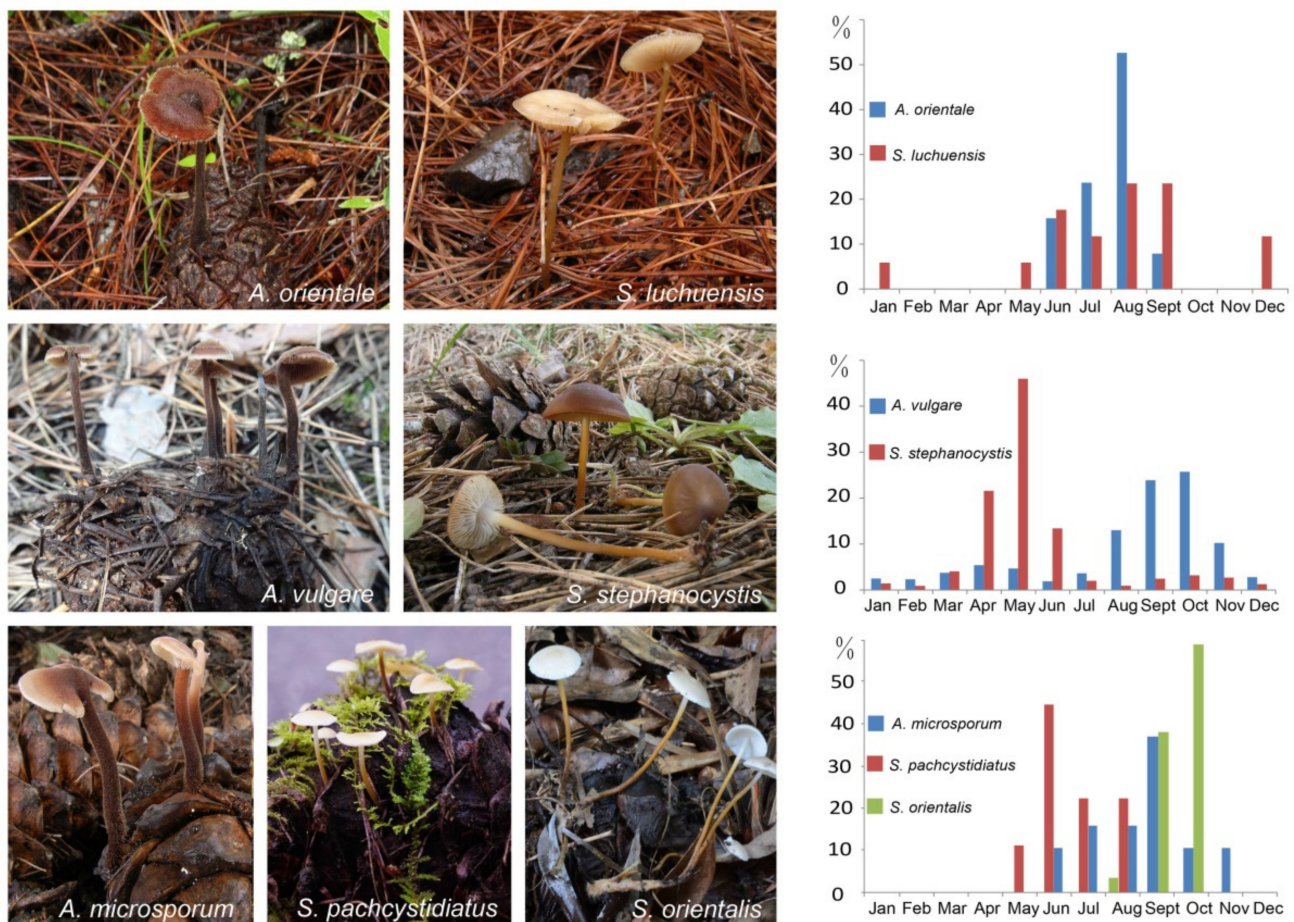


Figure 1. Basidiomata and percentage of monthly occurrences of fruiting bodies of *Auriscalpium* and *Strobilurus* on pinecones. The basidiomata of *Auriscalpium* usually on newly fallen cones on the ground. The basidiomata of *Strobilurus* usually on highly rotten cones under the ground. For the graphs, the x-axis shows months and the y-axis shows percentage of monthly occurrences of collected or observed fruiting bodies on pinecones in different areas and years in Table S1.

The ecological characteristics of colonization and fruiting by *Auriscalpium* and *Strobilurus* fungi on pinecones as observed in the field were similarly found in our greenhouse fruiting experiment (Figure S2). There are hyphae or spores of *S. pachcystidiatus* and *S. orientalis* in the cones occupied by *A. microsporum* collected from the field. Under the greenhouse culture condition, fruiting bodies of *A. microsporum* formed first from July to September, then *S. pachcystidiatus* appeared from May to July over the next 3 years, and finally *S. orientalis* appeared from October to December. Together, these greenhouse observations are consistent with our field observations on the ecological successions of these fungi on pinecones (Figure S2). However, because the environmental humidity in the greenhouse is stable, the fruiting time of fungi in *Auriscalpium* and *Strobilurus* is relatively continuous.

3.2. Genome Sequencing, Data Preprocessing, Assembly, General Genome Features, Protein-Coding Gene Prediction and Functional Annotation

The general features of the seven genomes that we sequenced are summarized in Table 1. Raw data were generated with Pacbio sequencing and Illumina sequencing with coverage $85.84\text{--}386.08\times$ and $101.04\text{--}206.85\times$, respectively (Table S2). Among the *Auriscalpium* species, *A. vulgare* had the largest genome (51.68 Mb), followed by *A. orientale* (45.40 Mb), and *A. microsporum* had the smallest genome (43.46 Mb) (Table 1). Among the

species of *Strobilurus*, *S. pachycystidiatus* had the largest genome (51.82 Mb), followed by *S. orientalis* (51.25 Mb) and *S. luchuensis* (46.71 Mb), and *S. stephanocystis* had the smallest genome (42.38 Mb) (Table 1). The sets of annotated protein-coding genes in the seven assembled genomes were estimated to be 92.4–100% complete (Table S3). Among the *Auriscalpium* species, *A. orientale* had the most coding genes (16,958), followed by *A. microsporium* (15,333), and *A. vulgare* had the least coding genes (13,636). Among the taxa of *Strobilurus*, *S. orientalis* has the most coding genes (18,509), followed by *S. pachycystidiatus* (18,157) and *S. luchuensis* (16,796), and *S. stephanocystis* had the least number of coding genes (16,439).

Table 1. The characteristics of the assembly scaffold and genomes of three *Auriscalpium* species and four *Strobilurus* species.

	<i>A. vulgare</i>	<i>A. microsporium</i>	<i>A. orientale</i>	<i>S. stephanocystis</i>	<i>S. pachycystidiatus</i>	<i>S. luchuensis</i>	<i>S. orientalis</i>
Strain No.	CBS 236.39	A-H-210-14	A-Y-A	CBS 113577	Y-H-6C	Y-Y-2D	K-1-1
Number of Contigs	104	54	38	38	71	58	43
Length of the genome assembly (Mb)	51.68	43.46	45.40	42.38	51.82	46.71	51.25
Contig N50 (Mb)	1.721	2.449	1.814	2.875	2.269	2.554	3.397
GC content (%)	56.39	56.13	56.68	52.13	51.75	51.76	51.53
Number of protein-coding genes	13,639	15,333	16,958	16,439	18,157	16,796	18,509
Median/Average gene length (bp)	1716/2202	1862/2246	1886/2300	1702/2033	1736/2139	1732/2116	1747/2146
Median/Average coding sequence size (bp)	1392/1675	1508/1801	1535/1867	1441/1721	1446/1754	1467/1761	1471/1787
Median/Average number of exons per gene	5/5.8	6/7.1	6/7.3	5/6.7	5/6.7	5/6.7	5/6.8
Median/Average exon size (bp)	172/288	144/252	140/257	143/256	148/263	150/265	146/262
Median/Average intron size (bp)	55/109	55/71	55/67	52/53	52/67	52/62	52/60
Median/Average size of intergenic regions (bp)	674/1544	399/1085	386/953	396/893	454/1086	462/1065	449/1046
Gene density (genes/Mbp)	264	353	374	388	350	360	361

3.3. Identification of CAZymes and Lignocellulolytic Genes in Fungi of *Auriscalpium* and *Strobilurus*

The number of CAZymes in *A. vulgare*, *A. microsporium*, *A. orientale*, *S. stephanocystis*, *S. luchuensis*, *S. pachycystidiatus* and *S. orientalis* were 450, 425, 464, 532, 542, 583 and 621, respectively (Figure 2b; Table S4). Our statistical analyses revealed that the average number of CAZymes in *Auriscalpium* fungi is significantly lower than that in *Strobilurus* such as AA5, CBM18, CBM67, CE12, CE16, CE4, CE8, GH105, GH12, GH127, GH128, GH13, GH135, GH16, GH17, GH18, GH27, GH28, GH29, GH35, GH43, GH45, GH5, GH53, GH55, GH71, GH76, GH93, GT1, GT15, GT17, GT33, GT4, GT8, PL1 and PL4 (Table S5). The average number of CAZymes in *Auriscalpium* fungi is significantly more than that in *Strobilurus* only in seven gene families including AA2, GH2, GH3, GH15, GH31, GH109 and PL8 (Table S5). Similarly, in the statistical analyses, the comparison of CAZymes between *Auriscalpium* and other WR fungi, and the comparison of CAZymes between *Strobilurus* and other WR fungi are shown in Table S6 and S7, respectively. The average number of CAZymes in *Auriscalpium* fungi is significantly more than that in other WR fungi only

in six gene families, however the average number of CAZymes in *Strobilurus* fungi is significantly more than that other WR fungi in 31 gene families (Tables S6 and S7).

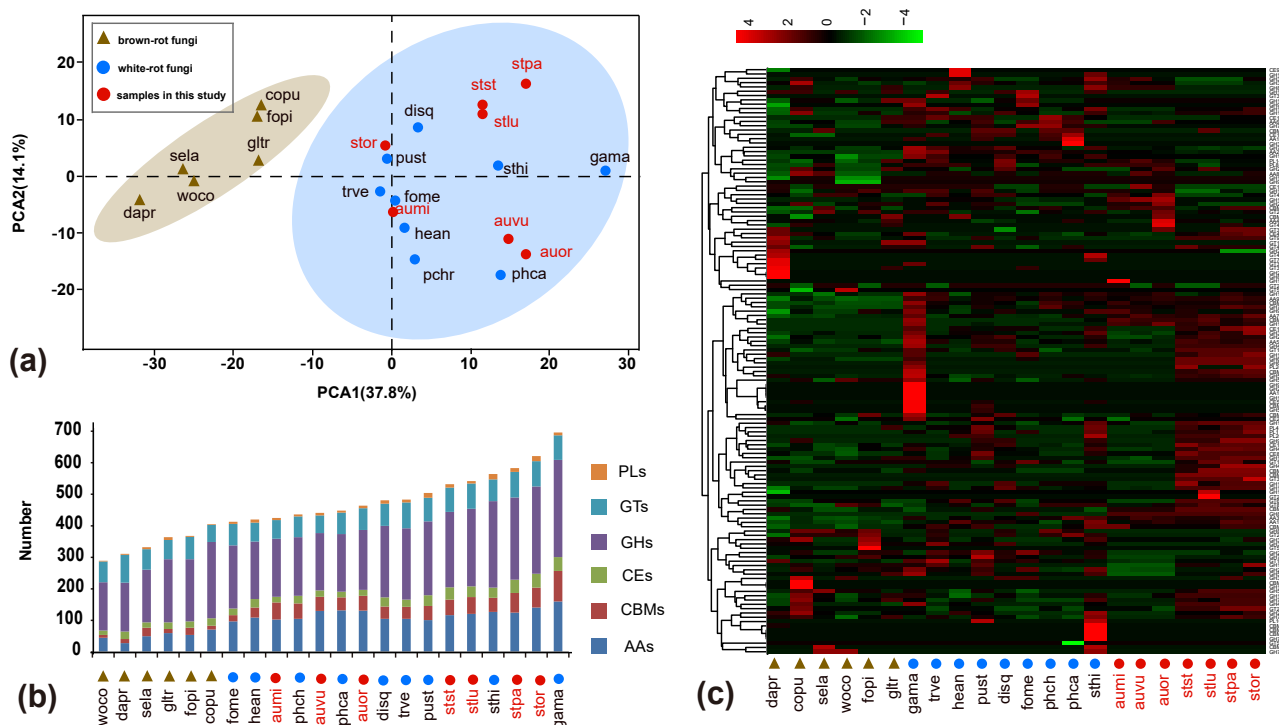


Figure 2. The distributions of genes encoding carbohydrate-active enzymes (CAZymes) in *Auriscalpium* and *Strobilurus* fungi. (a) wood decay fungi (WDF) plotted on the first two principal components from principal component analyses (PCA) of CAZymes. (b) Comparative analyses of CAZymes associated with lignocellulose decomposition. AAs: Auxiliary Activities; CBMs: Carbohydrate-Binding Modules; CEs: Carbohydrate Esterases; GHs: Glycoside Hydrolases; GTs: Glycosyl Transferases; PLs: Polysaccharide Lyases. (c) Heatmap analysis of CAZymes showing the distributions of CAZymes among different fungi. Numbers of family members in each genome are demonstrated. Overrepresented (+4 to 0) and underrepresented (0 to −4) numbers are depicted as scores for each line in heatmap. The clustering on the left involves gene families with the same pattern in number. On the right is the name of the gene family.

The number of predicted lignocellulolytic genes in *A. vulgare*, *A. microsporum*, *A. orientale*, *S. stephanocystis*, *S. luchuensis*, *S. pachycystidiatus* and *S. orientalis* were 112, 97, 111, 107, 106, 122 and 111, respectively (Table S8). Our analyses demonstrated that the number of genes coding for AA2, GH3 and GH7 in *Auriscalpium* are significantly higher than those in *Strobilurus*, while the number of genes coding for AA1, CE8, GH12, GH5_5, GH45 and PL1_4 in *Strobilurus* are significantly higher than those in *Auriscalpium* (Table S9). For the fungi growing on cones of the same pine species, the proportions of genes encoding ligninases and hemicellulases were higher in *Auriscalpium* species than those in their corresponding *Strobilurus* species. In contrast, the proportions of genes encoding cellulases and pectinases were lower in *Auriscalpium* than those in the *Strobilurus*. For fungi living on cones of *P. armandii*, *A. microsporum* and *S. pachycystidiatus* living on relatively newly fallen cones also showed a similar pattern but the difference was less obvious than those in other two fungal pairs. However, *S. orientalis* with a preference of living on more rotten cones showed more obvious differences in their respective enzymes compared with *A. microsporum*.

3.4. PCA and Heatmap Analyses of CAZymes and Lignocellulolytic Genes

Results of the PCA of CAZymes and lignocellulolytic genes showed a clear separation of WR and BR fungi along PCA1 (Figure 2a and Figure S4a). All the fungi in *Auriscalpium*

and *Strobilurus* cluster together with other WR fungi, consistent with their potent lignin-decomposing ability (Figure 2a and Figure S4a). The heatmap analyses showed that there are unique enzymes within each of the 22 fungi analyzed, which likely reflect the diversity of their preferred substrates (Figure 2c and Figure S4b). In the separate analyses of the two genera, it is apparent that fungi in the two genera showed complementary profiles of carbohydrate-active enzymes (CAZymes) (Figures 3a and 4g,h). The results clearly illustrate that there are remarkable differences in the overall pattern of genes between two different genera. At the same time, it demonstrates that the type and number of these CAZymes in *Auriscalpium* and *Strobilurus* are different among different fungi, which may partly explain the cause of the substrate specificity (Figure S5a,b). The results of the lignocellulolytic genes are overall consistent with the results of CAZymes (Figure S5c,d). These lignocellulolytic genes are also specific among genera, and there are great differences in the type and number of enzymes among different genera, and each has a set of different enzyme system (Figure 4g,h and Figure S5c,d).

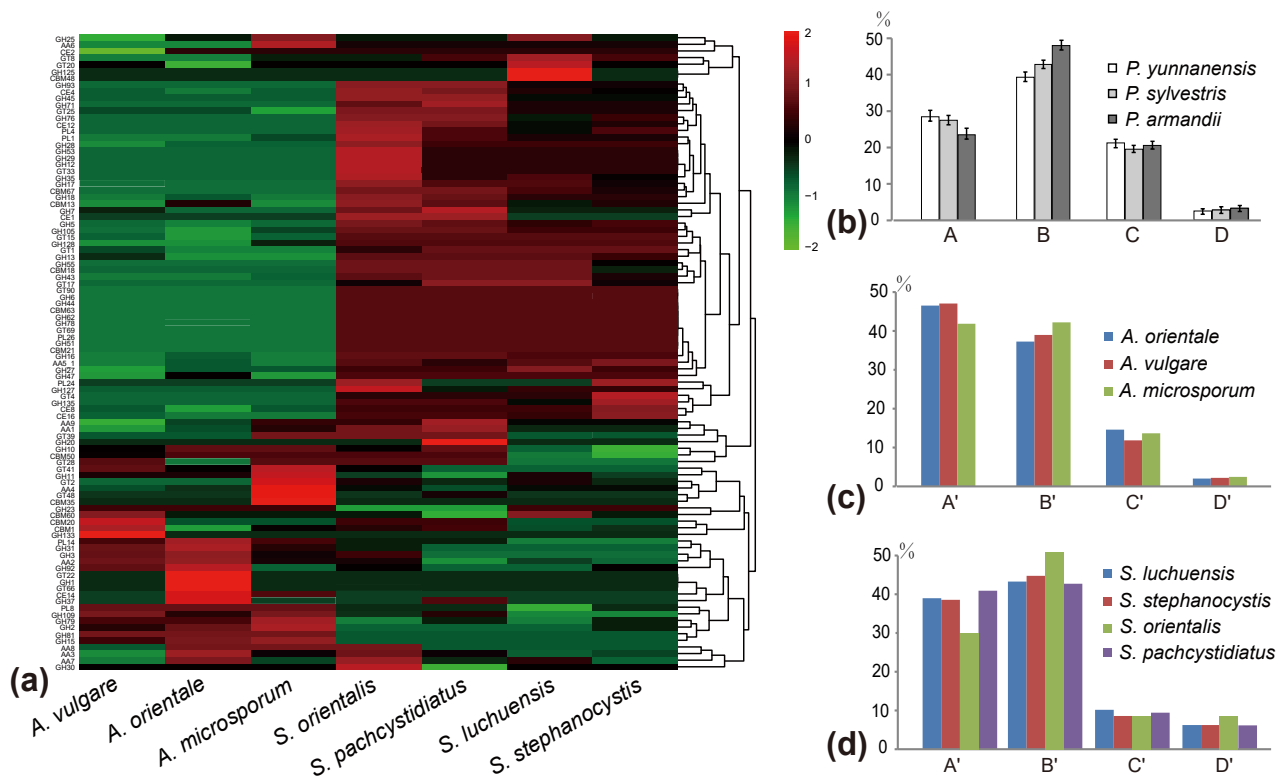


Figure 3. Comparisons of the carbohydrate-active enzymes (CAZymes) in *Auriscalpium* and *Strobilurus*, the proportions of four major chemical components in different cones, and the proportions of different enzymes encoded by lignocellulolytic genes in the two fungi groups. (a) Heatmap analysis of seven fungi in *Auriscalpium* and *Strobilurus* of CAZymes. (b) Four components of three different newly fallen cones. A, B, C and D in x-axis represent lignin, cellulose, hemicellulose and pectin, respectively. The y-axis represents the proportion of the four components. (c) The proportions of lignocellulolytic genes in different fungi of *Auriscalpium*. A', B', C', D' in x-axis represent ligninase, cellulase, hemicellulase, pectinase, respectively. The y-axis represents the proportion of the four types of enzymes; the same below. (d) The proportions of lignocellulolytic genes in different fungi of *Strobilurus*.

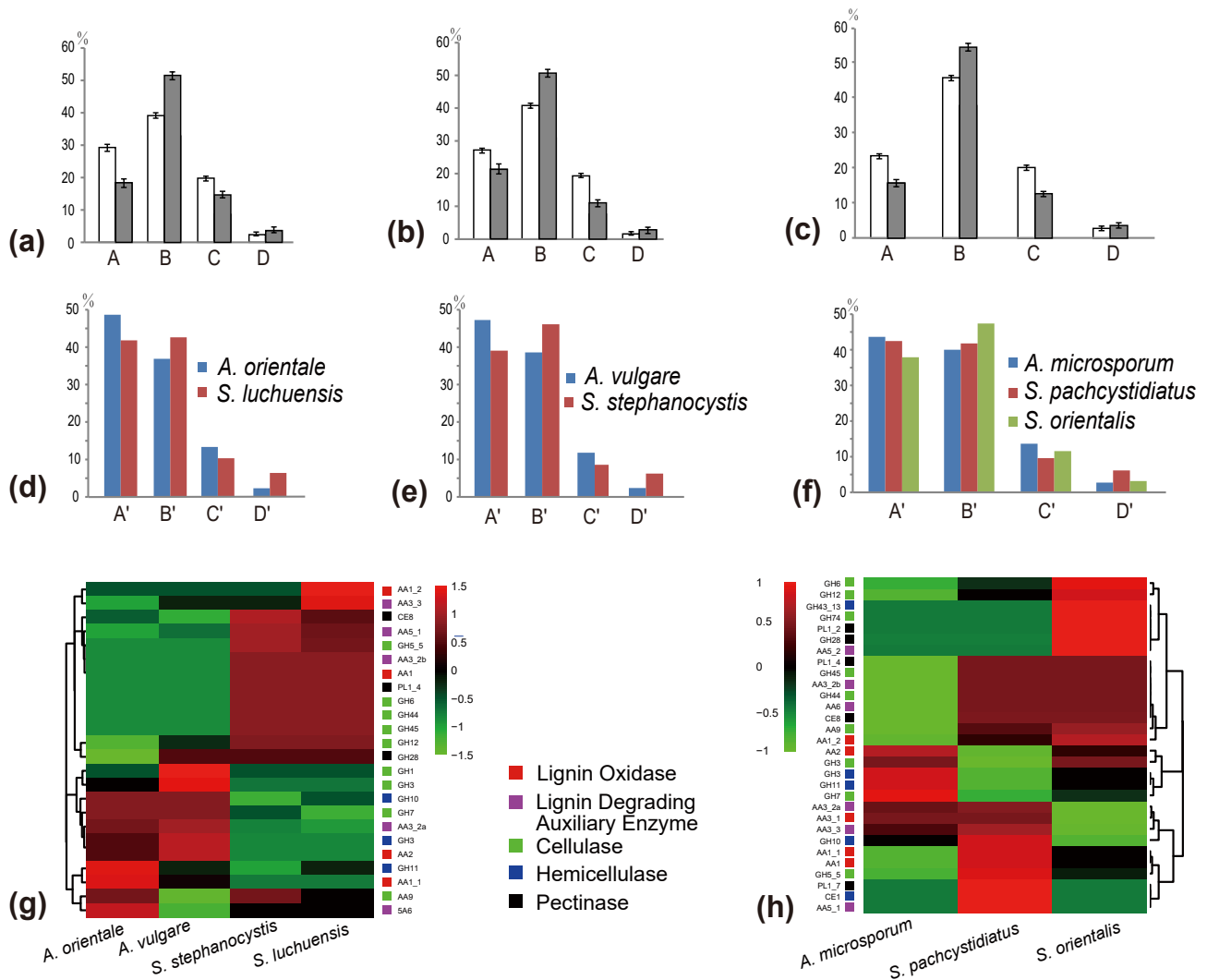


Figure 4. The changes of four major chemical components of cones before and after decomposition, and the relationship to differences of the numbers of lignocellulolytic genes between *Strobilurus* and *Auriscalpium* fungi colonizing the same pinecones. (a) The proportion of four components in cones of *P. yunnanensis* before and after the decomposition by *A. orientale*. A, B, C and D in x-axis represent lignin, cellulose, hemicellulose and pectin, respectively. The y-axis represents the proportion of the four components. White represents undecomposed cones, while gray represents decomposed cones. the same below. (b) The proportion of four components in cones of *P. sylvestris* before and after the decomposition by *A. vulgare*. (c) The content changes of four components in cones of *P. armandii* before and after being decomposed by *A. microsporum*. (d) Comparison of lignocellulolytic genes. A', B', C' and D' in x-axis represent ligninase, cellulose, hemicellulose and pectinase, respectively. The y-axis represents the proportion of the four types of enzymes in *A. orientale* and *S. luchuensis* grown on cones of *P. yunnanensis*. The same below. (e) Comparison of lignocellulolytic genes in *A. vulgare* and *S. stephanocystis* on cones of *P. sylvestris*. (f) Comparisons of lignocellulolytic genes of *A. microsporum*, *S. pachycystidiatus* and *S. orientalis* grown on cones of *P. armandii*. (g) Heatmap analysis of lignocellulolytic genes of four fungi on cones of *P.* subgenus *Pinus*. (h) Heatmap analysis of lignocellulolytic genes of three fungi on cones of *P.* subgenus *Strobus*.

3.5. Composition Analyses of Pinecones

Among newly fallen cones, that of *P. yunnanensis* showed the highest contents of lignin and hemicellulose, but the least amounts of cellulose and pectin. In contrast, the cones of *P. armandii* showed the highest contents of cellulose and pectin, but the least amount of lignin (Figure 3b; Table S10). In addition to the least amount of hemicellulose, the other components in the cone of *P. sylvestris* are between those in the cones of the other two species (Figure 3b; Table S10). Compared with the newly fallen cones, the

cones already decomposed by corresponding *Auriscalpium* fungi had reduced relative proportions of lignin and hemicellulose and increased relative proportions of cellulose and pectin (Figure 4a–c; Table S10).

3.6. Enzymes Related to Resin Decompositions

Among the top 10 enzymes showing elevated expressions in the presence of latex in *R. microporus*, our analyses revealed that four of them had an overall greater numbers of genes coding for these enzymes in *Auriscalpium* fungi than in *Strobilurus* in the top No. 1, 2, 6 and 10 in *Auriscalpium* is more than those in *Strobilurus* (Table 2). Overall, among all the genes, the number of genes coding for peptidase S8 (No. 1) and peptidase S53 (No. 6) in *Auriscalpium* were significantly higher than that in *Strobilurus* ($p < 0.05$), while the other genes were not significantly different. Of the genes coding for peptidase S8, the average number in *Auriscalpium* is 20.33, while only 5.4 in *Strobilurus* (Table 2). In genes coding for peptidase S53, the average numbers in *Auriscalpium* and *Strobilurus* were 3.7 and 1.2, respectively (Table 2).

3.7. SM Clusters in *Strobilurus* and *Auriscalpium*

Terpenes, NRPS (nonribosomal peptide synthetase)-like compounds, and siderophores are among the main groups of SMs shared by fungi in *Auriscalpium* and *Strobilurus* and the putative genes coding for enzymes involved in their syntheses are summarized in Table 3. Our analyses showed that T1PKS (type I polyketide synthases)-NRPS like and betalactone existed solely in *Auriscalpium*, while T1PKS-terpene, strobilurin, T1PKS, and indole alkaloids were only found in *Strobilurus* (Table 3). Our results revealed that the average number of gene clusters for SMs in *Auriscalpium* fungi was fewer (average 18.33) than that in *Strobilurus* (average 21.25). As expected, each species of *Strobilurus* harbors one SM clusters of strobilurin (Table 3). Fungi in *Auriscalpium* contain very few gene clusters for NRPS-like but abundant for terpenes, while fungi in *Strobilurus* are the opposite (Table 3). In summary, the number of genes predicted for the synthesis of NRPS-like, T1PKS, strobilurin and indole alkaloids in *Strobilurus* fungi is higher than those in *Auriscalpium* taxa.

3.8. Result of Species Tree Construction, Divergence Time Estimation and Gene Family Expansions of CAZymes Analysis

Maximum-likelihood phylogenetic analysis using concatenated nucleotide sequences of the 1519 single-copy orthologs identified through OrthoMCL analysis present in all species of 22 fungi. Most of the nodes have high support rate, which proves that our phylogenetic tree can well analyze the phylogenetic and evolutionary relationship between species. The result of divergence time estimation is shown in Figure 5a.

Table 2. Abundance and distribution of the top 10 groups of overexpressed genes in the presence of latex among the seven sequenced genomes in this study.

	InterPro Hit ID	InterPro Hit Description	<i>S. luchuensis</i>	<i>S. pachycystidiatus</i>	<i>S. stephanocystis</i>	<i>S. orientalis</i>	<i>A. microsporium</i>	<i>A. orientale</i>	<i>A. vulgare</i>	<i>Strobilurus_mean</i>	<i>Auriscalpium_mean</i>	Padj †
1	IPR000209	Peptidase S8	6	4	5	4	19	23	20	4.75	20.67	0.021 *
2	IPR001461	Aspartic peptidase	17	17	16	19	18	34	28	17.25	26.67	0.432
3	IPR008972	Cupredoxin	8	8	7	7	9	5	7	7.5	7	0.889
4	IPR001128	Cytochrome P450	92	94	97	96	95	121	98	94.75	104.67	0.584
5	IPR018487	Hemopexin-like repeats	0	0	0	0	0	0	0	0	0	1
6	IPR015366	Peptidase S53	1	1	2	1	3	4	4	1.25	3.67	0.021 *
7	IPR001338	Hydrophobin	0	0	0	0	0	0	0	0	0	1
8	IPR001128	Cytochrome P450	31	22	27	37	20	23	28	29.25	23.67	0.432
9	IPR001338	Hydrophobin	4	9	4	11	6	6	6	7	6	0.876
10	IPR011701	Major facilitator superfamily	37	42	41	49	44	55	53	42.25	50.67	0.387

* significance at the level of $p < 0.05$. † adjusted p -value based on the False Discovery Rate (FDR) method for multiple testing correction.

Table 3. Comparison of secondary metabolisms of fungi in *Auriscalpium* and *Strobilurus*.

Secondary metabolisms	<i>S. stephanocystis</i>	<i>S. luchuensis</i>	<i>S. pachycystidiatus</i>	<i>S. orientalis</i>	<i>A. vulgare</i>	<i>A. orientale</i>	<i>A. microsporium</i>	<i>Strobilurus_mean</i>	<i>Auriscalpium_mean</i>
Terpene	7	8	8	9	13	13	8	8	11.33
T1PKS	0	0	1	0	0	0	0	0.25	0
†-Terpene	0	0	0	0	1	1	1	0	1
†-NRPS-like	10	9	9	7	6	1	4	8.75	3.67
NRPS †-like	2	1	1	1	1	2	1	1.25	1.33
Siderophore	0	0	0	0	1	1	1	0	1
betalactone	1	1	1	1	0	0	0	1	0
Strobilurin	1	1	0	2	0	0	0	1	0
T1PKS †	1	1	1	1	0	0	0	1	0
indole	1	1	1	1	0	0	0	1	0
total	22	21	21	21	22	18	15	21.25	18.33

† type I polyketide synthases. ‡ nonribosomal peptide synthetase.

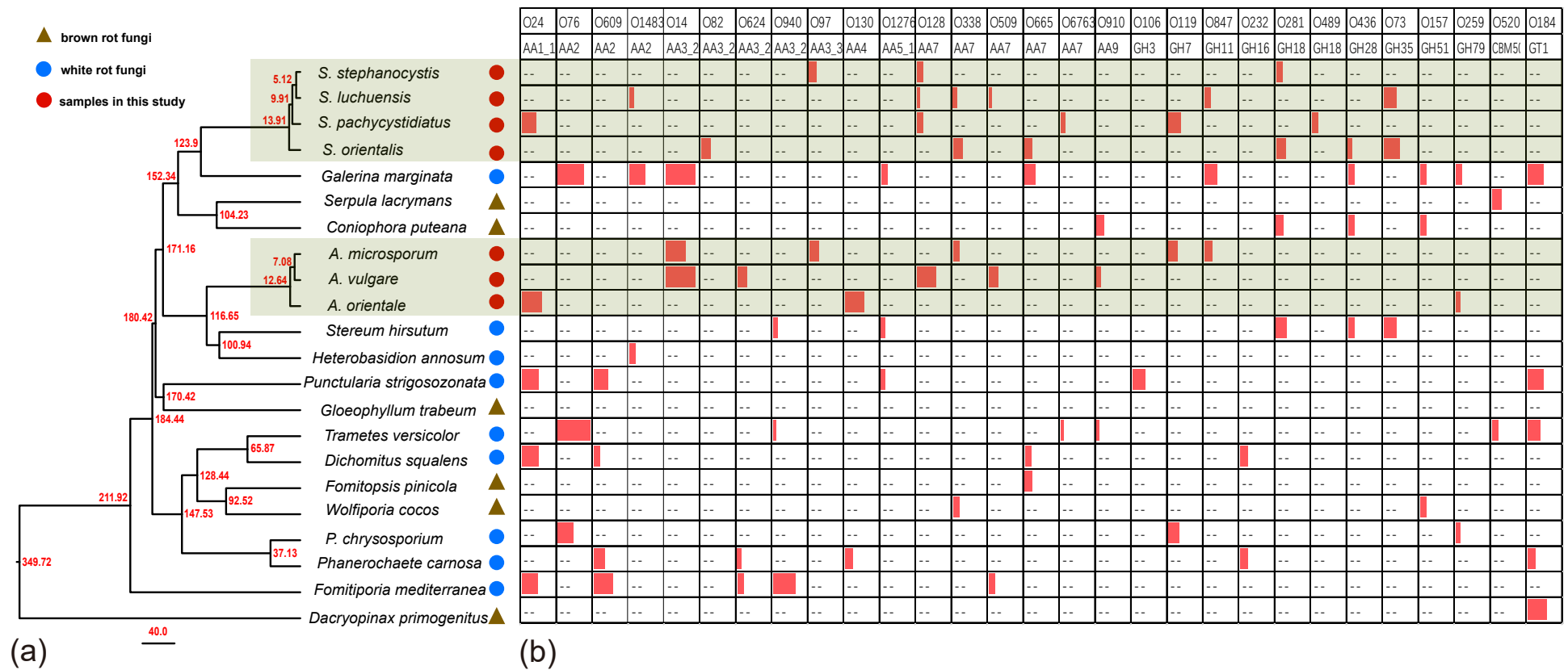


Figure 5. Phylogenetic tree of fungi in *Auriscalpium* and *Strobilurus* with other 15 fungal species and gene family expansions of CAZymes using CAFE. (a) The topology of the phylogenetic tree was constructed by the maximum likelihood method and divergence time estimation using r8s. Their divergence time was marked on the phylogenetic tree with time scale being shown by MYA (million years ago). (b) gene family expansions of CAZymes in 22 fungi with p-values less than 0.05. “O” in the first row of the table represents OCG (Ortholog Cluster Group); The second row of the table represents the gene family information of CAZymes. The length of the red rectangle represents the quantity; “--” represents that the gene family has not been significantly expanded in this species.

Among those expanded Ortholog Cluster Groups (OCGs) examined using CAFE since their most recent common ancestor (MRCA) bifurcated, *S. stephanocystis* contained 3 OCGs of CAZymes including OCG97 (AA3_3) (gene number (GM) 5), OCG128 (AA7) (GM 4) and OGC281 (GH18) (GM 4), *S. luchuensis* contained 6 OCGs of CAZymes including CG1483 (AA2) (GM 3), OCG128 (AA7) (GM 2), OCG338 (AA7) (GM 3), OCG509 (AA7) (GM 2), OCG847 (GH11) (GM 4) and OCG73 (GH35) (GM 8), *S. pachycystidiatus* contained 6 OCGs of CAZymes including OCG24 (AA1_1) (GM 9), OCG128 (AA7) (GM 4), OCG6763 (AA7) (GM 3), OCG 119 (GH7) (GM 8) and OCG489 (GH18) (GM 4), *S. orientalis* contained 6 OCGs of CAZymes including OCG82 (AA3_2) (GM 6), OCG338 (AA7) (GM 6), OCG665 (AA7) (GM 5), OCG281 (GH18) (GM 6), OCG436 (GH28) (GM 3) and OCG73 (GH35) (GM 10), *A. microsporum* contained 5 OCGs of CAZymes including OCG14 (AA3_2) (GM 13), OCG97 (AA3_3) (GM 6), OCG338 (AA7) (GM 4), OCG119 (GH7) (GM 6), and OCG847 (GH11) (GM 5), *A. vulgare* contained 5 OCGs of CAZymes including OCG14 (AA3_2) (GM 19), OCG624 (AA3_2) (GM 6), OCG128 (AA7) (GM 12), OCG509 (AA7) (GM 6), and OCG910 (AA9) (GM 3), and *A. orientale* contained 3 OCGs of CAZymes including OCG24 (AA1_1) (GM 13), OCG130 (AA4) (GM 12), and OCG259 (GH79) (GM 3) (Figure 5b; Table S11). Those expanded OCGs of other species shown in Figure 5b and Table S11.

4. Discussion

4.1. Successive Decomposition of Pinecones by Fungi of *Auriscalpium* and *Strobilurus*

The successive decomposition of substrates by microbial communities is a common phenomenon [28,62]. Often, the microbial community structure, including the relative abundances of saprotrophic fungi, changes significantly during the successive decomposition process [63]. Though occupying the same ecological niche, species in these communities may develop unique but complementary strategies to partition the resources in the substrates, leading to temporal niche differentiation and divergence [64]. Here, part of the resource partition is temporal changes of fungi with different fungi use different sets of nutrients within the pinecone. Similar phenomena have been found in other substrates such as plant litters and deadwoods [3,13,65]. In the process of biodegradation, microbial coordination with different ecological strategies and certain orders are evident [65,66]. For example, successions of fungi in temperate forests were considered to be reflected in sugar utilizing fungi, followed by wood structural decaying fungi and finally residual decaying fungi in some cases [67]. This change may be explained in part by nutrients released by the primary decomposers that enabled the colonization of secondary decomposers [7]. However, the successive decomposition of substrates, such as deadwood and plant litter, requires the action and interaction of many fungi with their fungal community showing a high degree of complexity [3,68]. For example, Zhang and Wei [29] had carried out relevant research on fungi in the same forest, in which different fungi will appear on rotten wood in the same state, or even on the same rotten wood. At the same time, the same kind of fungi can also exist in different periods of rotten wood (Figure S1). Some fungi can only appear in one period, but most fungi can produce fruiting bodies at several stages of rotten wood [29], Figure S1. Similarly, Niemela et al. [28] reported the succession of more than one hundred species of lignicolous Basidiomycetes on fallen trunks in *Picea obovata* and *P. sylvestris*. Our study revealed that fungi in *Auriscalpium* and *Strobilurus* possess clear differences in the type and number of CAZymes and lignocellulolytic genes (Figure 2c, Figure 3a, Figure 4g,h and Figure S4b). Our results indicate that even though they colonize the same pinecones, there are significant divergence and niche differentiation in the utilization of substrates in pinecones between the fungi of the two genera, which leads to the dynamic changes of their colonization on the pinecones.

During the initial decomposition of pinecones, *Auriscalpium* fungi are the primary colonizers, likely related to their ability to break down resin and their strong capacity to decompose lignin and hemicellulose (Figure 4a–c; Table 2). Such abilities are common among WR fungi [69]. For example, the fungi of *Ceriporiopsis subvermispora*, *Phellinus pini*, *Ganoderma australe*, and *Phlebia tremellosa* specifically degrade lignin and hemicellulose

among WR fungi [70]. The most compelling evidence supporting the early colonizing ability of *Auriscalpium* fungi is that their number of peptidases S8 and S53 is far greater than that in *Strobilurus* fungi. Peptidases S8 and S53 are among the top 10 most up-regulated enzymes in *R. microporus* in the presence of latex [50], Table 2. The genomic evidence is consistent with *Auriscalpium* fungi capable of colonizing newly fallen cones and decomposing proteins in resin rapidly. Polo et al. [71] showed that lignin and hemicellulose are in the outermost layer of plant cell wall which prevents the cellulolytic enzymes reaching the cellulose and protect plants from microbes. Our analyses demonstrated that the number of genes coding for lignin oxidases (AA2) and hemicellulase (GH3) in *Auriscalpium* are significantly higher than those in *Strobilurus* (Figure 4g,h; Table S9), and these genes may be related to lignin and hemicellulase decompositions in the outermost layer of pinecones. Similarly, in the analysis of gene family expansions, we found that the number of lignin related decomposition gene families was significantly higher in *Auriscalpium* than those of fungi in *Strobilurus*. For example, there are six gene families related to lignin decomposition expanded in *Auriscalpium*: *A. microsporum* including OCG14 (AA3_2) (GM 13) and OCG97 (AA3_3) (GM 6), *A. vulgare* including OCG14 (AA3_2) (GM 19) and OCG624 (AA3_2) (GM 6), and *A. orientale* including OCG24 (AA1_1) (GM 13) and OCG130 (AA4) (GM 12), while only four gene families related to lignin decomposition expanded in *Strobilurus*: *S. stephanocystis* including OCG97 (AA3_3) (GM 5), *S. luchuensis* including CG1483 (AA2) (GM 3), *S. pachycystidiatus* including OCG24 (AA1_1) (GM 9), and *S. orientalis* including OCG82 (AA3_2) (GM 6) (Figure 5b; Table S11). Once the outer layer is breached, the condition is now more favorable for the subsequent invasion of *Strobilurus* fungi. With increasing decay, the nutritional composition, physical structure, chemical composition and other aspects of the pinecones have changed, which result in the succession changes of fungal community.

After decomposition by *Auriscalpium* fungi, the proportions of lignin and hemicellulose in the pinecone would decrease and those of cellulose and pectin proportionally would increase (Figure 4a–c). The subsequent colonization by *Strobilurus* fungi relies on the residual components of the cones suitable for their growth and replacing the corresponding fungi of *Auriscalpium* (Figure 6). Similarly, comparing *Auriscalpium* and *Strobilurus* grown on the same pinecone, fungi of *Strobilurus* show decreasing trends of in the number of genes coding for ligninases and hemicellulases, but with higher number of genes coding for cellulase and pectinase, which is broadly consistent with the changes of cone components (Figure 4a–f). *Strobilurus pachycystidiatus* and *A. microsporum* also show the same pattern, but the differences are not particularly evident, which may relate to the fact that both could grow on newly fallen cones. However, *S. orientalis* grew on the highly rotten cones after decomposition by *A. microsporum* or *S. pachycystidiatus* and it showed a more obvious decrease in the number of ligninase-encoding genes and an increase in the number of cellulase-encoding genes than *S. pachycystidiatus* (Figure 4f). Accordingly, in the analysis of gene family expansions, we found that the number of GH gene families of fungi in *Strobilurus* was significantly higher than those of fungi in *Auriscalpium*. For example, there are eight gene families related to GH expanded in *Strobilurus*: *S. stephanocystis* including OGC281 (GH18) (GM 4), *S. luchuensis* including OCG847 (GH11) (GM 4) and OCG73 (GH35) (GM 8), *S. pachycystidiatus* including OCG 119 (GH7) (GM 8) and OCG489 (GH18) (GM 4), and *S. orientalis* including OCG281 (GH18) (GM 6), OCG436 (GH28) (GM 3) and OCG73 (GH35) (GM 10), while only three gene families related to GH expanded in *Auriscalpium*: *A. microsporum* including OCG119 (GH7) (GM 6), and OCG847 (GH11) (GM 5) and *A. orientale* including OCG259 (GH79) (GM 3) (Figure 5; Table S11). These gene families of GHs are related to the decomposition of cellulose, hemicellulose and pectin, respectively. For example, GH7 is related to cellulose decomposition, GH11 and GH35 are related to hemicellulose decomposition, and GH28 is related to pectin decomposition. All the above results show that the fungi in *Strobilurus* may have a good decomposition effect on utilizing the remaining organic compounds of the decomposed cones.

In addition, in the field, we observed that the fungi of *Auriscalpium* can decompose cones independently, especially in tropical areas, but the successive decomposition of the two genera is more common. However, we did not observe the decomposition of cones by fungi of *Strobilurus* independently. In each distribution areas of fungi in *Strobilurus*, fungi in *Auriscalpium* could be collected in different periods, and the fungi in *Strobilurus* collected all grow on the cones with high degree of decay. For successive decomposition of *P. armandii*'s cones, in addition to the most common combination of *A. microsporum*-*S. pachcystidiatus*-*S. orientalis*, we also observed the combinations of *A. microsporum*-*S. pachcystidiatus* and *A. microsporum*-*S. orientalis*. Therefore, various situations may occur in the field (Figure 6). Although *Strobilurus* fungi always appear on cones with a high degree of decomposition, however, the results of our field observation show that compared with *Auriscalpium* fungi, the *Strobilurus* fungi can occupy the cone for a long time and fully decompose the cone. There have been reports on the positive correlation between the large amount of CAZymes in the genome and the degradation of plant biomass [72], so we speculate that fungi in *Strobilurus* are the main decomposer with the type and number of CAZymes in *Strobilurus* being richer than those of *Auriscalpium* (Figure 2b,c and Figure 3a). In the CAZymes comparisons between the two genera, only seven CAZyme gene families have significantly more genes in the *Auriscalpium* fungi than in *Strobilurus*, while the other 36 gene families have more genes in *Strobilurus* fungi than in *Auriscalpium* fungi (Table S5), which broadly supports that the subsequent decomposers are main components of substrate decompositions [17].

4.2. Fungal Competition of *Auriscalpium* and *Strobilurus* on Pinecones

Successive decomposition may be affected by fungal competition. Fungal competitions of *Auriscalpium* and *Strobilurus* on substrates correspond to the two functional types: primary resource capture and secondary resource capture, respectively [7], so that the two genera appear orderly on the cones. On newly fallen cones, there may be hundreds of fungi competing to colonize cones on the surface, which is similar to the situation reported in woods [73]. However, the most obvious obstacles for fungi on newly fallen cones are the lack of easily assimilated nutrient matrixes such as lignin and hemicellulose, and the presences of inhibitory substances such as resin, etc. [74]. Due to their ability to breakdown these resistant substances, *Auriscalpium* can gain a competitive edge with other microorganisms in microbial community on newly fallen cones.

With the increase of the decomposition levels, the competitive pressures on the cones gradually increase attributed to the disappearance or reduction of antibacterial or antifungal substances. On one hand, the cones decomposed by the *Auriscalpium* provide suitable conditions for *Strobilurus* growth. During this period, the fruiting bodies of *Strobilurus* and *Auriscalpium* can co-exist on the same cone (Figure S3). On the other hand, fungi of *Strobilurus*, as aggressive competitors, produce toxins (e.g., strobilurin) to enhance its competitiveness with *Auriscalpium* and other microorganisms (Figure S3). For nutrients and spaces, the antagonists can either interact directly with the competitors [75], or secrete antibiotics to suppress competitors [76]. Some studies on antifungal SMs and enzymes produced by fungi with antagonists have been conducted extensively in vitro [77,78]. Through SM clusters analyses, we find that the number of SM clusters of the genus *Auriscalpium* is fewer than that of *Strobilurus* (Table 3), while all fungi of *Strobilurus* contain a fungicidal strobilurin cluster whose derivatives have broad spectrum antifungal activity, and, thus, are widely used as biological fungicide [79]. In addition, the number of NRPS-like in the genomes of *Strobilurus* is higher than those in *Auriscalpium* (Table 3). Most of the NRPS, PKS and their combinations have antibacterial and antifungal activities [80], which indicates that the fungi in *Strobilurus* have stronger antibacterial and antifungal activities than those in *Auriscalpium*. Aside from the SMs, other factors such as microclimate, the size and quality of nutrient sources can shift the balance between fungal decomposer groups [7]. Thus, in the natural environment, the outcomes of interactions between fungi are variable, leading to differences in community structures.

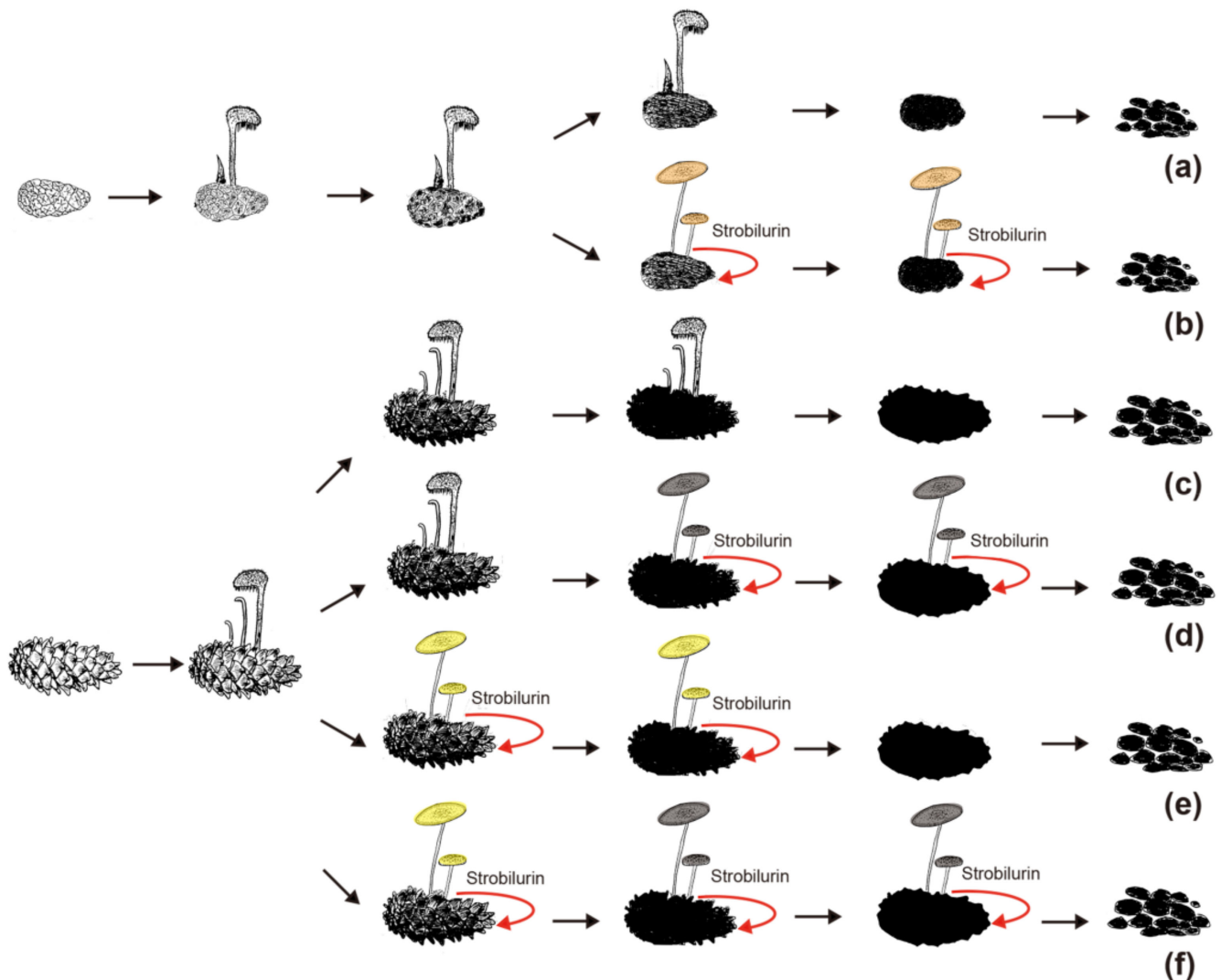


Figure 6. Types of successive decomposition of pinecones observed in the field. (a,b) The decomposition of cones of *P. subgenus Pinus*. (a) The cones decomposed by *A. vulgare* or *A. orientale* independently. (b) Successive decomposition and competition of *A. orientale*/*S. luchuensis* and *A. vulgare*/*S. stephanocystis* on cones of *P. subgenus Pinus*. The yellow brown pileus represents *S. luchuensis* or *S. stephanocystis*. (c–f) The decomposition of cones of *P. subgenus Strobus*. (c) The cones decomposed by *A. microsporum* independently. (d) Successive decomposition and competition of *A. microsporum* and *S. orientalis* on cones of *P. subgenus Strobus*. The gray brown pileus represents *S. orientalis*. (e) Successive decomposition and competition of *A. microsporum* and *S. pachcystidiatus* on cones of *P. subgenus Strobus*. The yellow pileus represents *S. pachcystidiatus*. (f) Successive decomposition and competition of *A. microsporum*, *S. pachcystidiatus* and *S. orientalis* on cones of *P. subgenus Strobus*.

5. Conclusions

Our results reveal that there are differentiations of temporal and trophic niches for fungi of *Auriscalpium* and *Strobilurus*. The decompositions of pinecones are frequently completed by these two groups of fungi through successive colonization, occupying the same physical niche but at different times. The primary colonizers were the fungi of *Auriscalpium* and the secondary ones were *Strobilurus* (Figure 6). The CAZymes of the two groups of fungi are highly unique but also complementary, leading to the complete biodegradation pinecones. For future research directions, we will clearly delineate successional timelines between *Auriscalpium* and *Strobilurus* to inform the mechanisms of successional decomposition through controlling expression profiles based on these timelines. Further associating

these profiles with realized relative loss in the cones over the time course has the potential to link critical successional dynamics to functional outcomes.

Supplementary Materials: The following are available online at <https://www.mdpi.com/article/10.3390/jof7080679/s1>, Figure S1: The distribution characteristics of wood decay fungi in different degrees of decay in Fenglin Nature Reserve (data from Zhang and Wei 2016). For the graphs, the *x*-axis shows different species and the *y*-axis shows number of occurrences of collected or observed fruiting bodies on wood in different years in Fenglin Nature Reserve. Different colors represent different levels of decay, and lengths represent numbers, Figure S2: The successive decomposition of *Pinus armandii* cones by *Auriscalpium* and *Strobilurus*. (a–b) *A. microsporum* fruiting from 2017 to 2019. (c–d) *S. pachycystidiatus* fruiting from 2018 to 2020. (e–f) *S. orientalis* fruiting from 2019 to now, Figure S3: The successive decomposition of cones by *Auriscalpium* and *Strobilurus* in the field. (a) *Auriscalpium* (white arrow) and *Strobilurus* (red arrow) on cone of *P. armandii*. (b–f) *Auriscalpium* (white arrow) and *Strobilurus* (red arrow) on cone of *P.* subgenus *Pinus*, Figure S4: The abundance and distributions of lignocellulolytic genes of *Auriscalpium* and *Strobilurus* demonstrated by multidimensional clustering approaches. (a) wood decay fungi (WDF) plotted on the first two principal components from principal component analyses (PCA) of lignocellulolytic genes. (b) Heatmap analysis of lignocellulolytic genes Numbers of family members in each genome are shown. Overrepresented (+4 to 0) and underrepresented (0 to −4) numbers are depicted as scores for each line in heatmap. The clustering on the left involves gene families with the same pattern in number. On the right is the name of the gene family, Figure S5: Analyses of carbohydrate-active enzymes (CAZymes) and lignocellulolytic genes within genera of *Auriscalpium* and *Strobilurus* derived from heatmap, and principal component analyses (PCA). (a) Heatmap analysis of three fungi of CAZymes in *Auriscalpium*. (b) Heatmap analysis of four fungi of CAZymes in *Strobilurus*. (c) Heatmap analysis of three fungi of lignocellulolytic genes in *Auriscalpium*. (d) Heatmap analysis of four fungi of lignocellulolytic genes in *Strobilurus*, Table S1: The collection information of fungi in *Auriscalpium* and *Strobilurus*, Table S2: Sequencing statistics, Table S3: Assessment of the protein gene set completeness in *Auriscalpium* and *Strobilurus* using BUSCO, Table S4: Gene distribution of carbohydrate-active enzymes (CAZymes) in *Auriscalpium* and *Strobilurus* fungi and the other 15 fungi, Table S5: Statistical analyses revealed that the average number of carbohydrate-active enzymes (CAZymes) in *Auriscalpium* and *Strobilurus* fungi, Table S6: The comparison of carbohydrate-active enzymes (CAZymes) between *Auriscalpium* and other WR fungi, Table S7: The comparison of carbohydrate-active enzymes (CAZymes) between *Strobilurus* and other WR fungi, Table S8: Gene distribution of lignocellulolytic genes in *Auriscalpium* and *Strobilurus* fungi and the other 15 fungi, Table S9: Statistical analyses revealed that the average number of lignocellulolytic genes in *Auriscalpium* and *Strobilurus* fungi, Table S10: Raw data of four major chemical components of cones before and after decomposition by fungi in *Auriscalpium*, Table S11: Gene family expansion of CAZymes in 22 fungi. Table S12: gff3 files of fungi in *Auriscalpium* and *Strobilurus*. Table S13: functional annotation of predicted gene models of fungi in *Auriscalpium* and *Strobilurus* based on similarity to annotated genes.

Author Contributions: Z.L.Y. designed the research and revised the manuscript; P.W. performed experiments, analyzed the data and wrote the manuscript; J.X. and G.W. provided help and advice, and revised the manuscript; T.L. provided samples for investigated the chemical compositions of pinecones. All authors have read and agreed to the published version of the manuscript.

Funding: The present research work was supported by the Strategic Priority Research Program of Chinese Academy of Sciences (XDB31000000) and Yunnan Ten-Thousand-Talents Plan-Yunling Scholar Project.

Institutional Review Board Statement: Not applicable.

Informed Consent Statement: Not applicable.

Data Availability Statement: The genomic data of our study were deposited in DDBJ/EMBL/GenBank including the *A. vulgare* (Accession number: JAHBBC000000000; BioProject: PRJNA728955; BioSample: SAMN19107592), *A. microsporum* (Accession number: JAHLMG000000000; BioProject: PRJNA735801; BioSample: SAMN19598194), *A. orientale* (Accession number: JAHLMH000000000; BioProject: PRJNA735804; BioSample: SAMN19598576), *S. luchuensis* (Accession number: JAHLMJ000000000; BioProject: PRJNA735851; BioSample: SAMN19599093), *S. pachycystidiatus* (Accession number: JAHLMK000000000; BioProject: PRJNA735855; BioSample: SAMN19599128), *S. stephanocystis* (Accession number: JAHLMI000000000; BioProject: PRJNA735844; BioSample: SAMN19598582) and *S. orientalis* (Accession number: JAHMLL000000000; BioProject: PRJNA735858; BioSample: SAMN19599131).

Acknowledgments: We are grateful to Fungal Biodiversity Centre in Netherlands (CBS) for providing us cultures of *Auriscalpium* and *Strobilurus*. We thank Xiang-Hua Wang, Hong Luo, Yan-Chun Li, Zai-Wei Ge, Feng Bang, Qing Cai, Jiao Qin, Qi Zhao, Xiao-Bin Liu, Xin Xu, Kui Wu, Hu Sun, Sheng-Wen Zhou, Cong Huang, Yi-Feng An, Jian-Yun Wu, Hua Qu, Peng-Cheng Yuan, and Jian-Wei Liu and Mei-Xiang Li, Xiao-Xia Ding (KIB), Xiao-Dan Yu (Shenyang Agricultural University), Tolgor Bau (Jilin Agricultural University), Ping Zhang (Hunan Normal University), Li-Hong Han (Qufu Normal University), Yan-Jia Hao (Anhui Normal University), Shi-Bin Jiao, De-Xian Kong for having provided us samples/specimens, collection information and/or color images. We thank Francis M. Martin (National Research Institute for Agriculture, Food and Environment, France), Li-Hong Han (Qufu Normal University), Hong Luo, Bang Feng, Qing Cai (KIB) and Shao-Xing Chen (Anhui Agricultural University), Xiao-Na Shao (Xishuangbanna Tropical Botanical Garden), Yan-Jia Hao (Anhui Normal University) and Jiao Qin (KIB) for their constructive and illuminating comments, criticisms and valuable suggestions. We appreciate Lian-Fu Chen, Xiao-Bin Liu for valuable information on data analysis.

Conflicts of Interest: The authors declare no conflict of interest.

References

- García-Palacios, P.; McKie, B.G.; Handa, I.T.; Frainer, A.; Hättenschwiler, S. The importance of litter traits and decomposers for litter decomposition: A comparison of aquatic and terrestrial ecosystems within and across biomes. *Funct. Ecol.* **2016**, *30*, 819–829. [[CrossRef](#)]
- Giweta, M. Role of litter production and its decomposition, and factors affecting the processes in a tropical forest ecosystem: A review. *J. Ecol. Environ.* **2020**, *44*, 11. [[CrossRef](#)]
- Baldrian, P.; Zrustová, P.; Tláskal, V.; Davidová, A.; Merhautová, V.; Vrka, T. Fungi associated with decomposing deadwood in a natural beech-dominated forest. *Fungal Ecol.* **2016**, *23*, 109–122. [[CrossRef](#)]
- Katagiri, S.; Shiba, T.; Tohara, H.; Yamaguchi, K.; Hara, K.; Nakagawa, K.; Komatsu, K.; Watanabe, K.; Ohsugi, Y.; Maekawa, S.; et al. Re-initiation of oral food intake following enteral nutrition alters oral and gut microbiota communities. *Front. Cell. Infect. Microbiol.* **2019**, *9*, 434. [[CrossRef](#)]
- Eichlerová, I.; Homolka, L.; Žifčáková, L.; Lisá, L.; Dobiášová, P.; Baldrian, P. Enzymatic systems involved in decomposition reflects the ecology and taxonomy of saprotrophic fungi. *Fungal Ecol.* **2015**, *13*, 10–22. [[CrossRef](#)]
- Rajala, T.; Peltoniemi, M.; Hantula, J.; Mäkipää, R.; Pennanen, T. RNA reveals a succession of active fungi during the decay of Norway spruce logs. *Fungal Ecol.* **2011**, *4*, 437–448. [[CrossRef](#)]
- Boddy, L. Interspecific combative interactions between wood-decaying basidiomycetes. *FEMS Microbiol. Ecol.* **2000**, *31*, 185–194. [[CrossRef](#)]
- Moor, H.; Nordén, J.; Penttil, R.; Siitonen, J.; Snll, T. Long-term effects of colonization-extinction dynamics of generalist versus specialist wood-decaying fungi. *J. Ecol.* **2020**, *109*, 491–503. [[CrossRef](#)]
- Krah, F.S.; Seibold, S.; Brandl, R.; Baldrian, P.; Müller, J.; Bässler, C. Independent effects of host and environment on the diversity of wood-inhabiting fungi. *J. Ecol.* **2018**, *106*, 1428–1442. [[CrossRef](#)]
- Rajala, T.; Peltoniemi, M.; Pennanen, T.; Mäkipää, R. Relationship between wood-inhabiting fungi determined by molecular analysis (DGGE) and quality of decaying logs. *Can. J. For. Res.* **2010**, *40*, 2384–2397. [[CrossRef](#)]
- Šnajdr, J.; Cajthaml, T.; Valášková, V.; Merhautová, V.; Petráňková, M.; Spetz, P.; Leppänen, K.; Baldrian, P. Transformation of *Quercus petraea* litter: Successive changes in litter chemistry are reflected in differential enzyme activity and changes in the microbial community composition. *FEMS Microbiol. Ecol.* **2011**, *75*, 291–303. [[CrossRef](#)]
- Riley, R.; Salamov, A.A.; Brown, D.W.; Nagy, L.G.; Floudas, D.; Held, B.W.; Lasseuse, A.; Lombard, V.; Morin, E.; Otilar, R.; et al. Extensive sampling of basidiomycete genomes demonstrate inadequacy of the white-rot/brown-rot paradigm for wood decay fungi. *Proc. Natl. Acad. Sci. USA* **2014**, *111*, 9923–9928. [[CrossRef](#)]
- Edman, M.; Eriksson, A.M. Competitive outcomes between wood-decaying fungi are altered in burnt wood. *FEMS Microbiol. Ecol.* **2016**, *92*, fiw068. [[CrossRef](#)] [[PubMed](#)]
- Edman, M.; Fällström, I. An introduced tree species alters the assemblage structure and functional composition of wood-decaying fungi in microcosms. *For. Ecol. Manag.* **2013**, *306*, 9–14. [[CrossRef](#)]

15. Fukami, T.; Dickie, I.; Wilkie, J.P.; Paulus, B.C.; Park, D.; Roberts, A.; Buchanan, P.K.; Allen, R.B. Assembly history dictates ecosystem functioning: Evidence from wood decomposer communities. *Ecol. Lett.* **2010**, *13*, 675–684. [[CrossRef](#)] [[PubMed](#)]
16. Sasha, V.; Bhatnagar, J.M. An evolutionary signal to fungal succession during plant litter decay. *FEMS Microbiol. Ecol.* **2019**, *95*, fiz145. [[CrossRef](#)]
17. Song, Z.W.; Vail, A.; Sadowsky, M.J.; Schilling, J.S. Competition between two wood-degrading fungi with distinct influences on residues. *FEMS Microbiol. Ecol.* **2012**, *79*, 109–117. [[CrossRef](#)]
18. Cantarel, B.L.; Coutinho, P.M.; Rancurel, C.; Bernard, T.; Lombard, V.; Henrissat, B. The Carbohydrate-Active EnZymes database (CAZy): An expert resource for glycogenomics. *Nucleic Acids Res.* **2009**, *37*, D233–D238. [[CrossRef](#)]
19. Kohler, A.; Kuo, A.; Nagy, L.G.; Morin, E.; Barry, K.; Buscot, F.; Canbäck, B.; Choi, C.; Cichocki, N.; Clum, A.; et al. Convergent losses of decay mechanisms and rapid turnover of symbiosis genes in mycorrhizal mutualists. *Nat. Genet.* **2015**, *47*, 410–415. [[CrossRef](#)]
20. Zhao, Z.; Liu, H.; Wang, C.; Xu, J.R. Comparative analysis of fungal genomes reveals different plant cell wall degrading capacity in fungi. *BMC Genom.* **2013**, *14*, 274. [[CrossRef](#)]
21. De Wit, P.J.G.M.; Van Der Burgt, A.; Ökmen, B.; Stergiopoulos, I.; Abd-Elsalam, K.A.; Aerts, A.L.; Bahkali, A.H.; Beenen, H.G.; Chettri, P.; Cox, M.P.; et al. The genomes of the fungal plant pathogens *Cladosporium fulvum* and *Dothistroma septosporum* reveal adaptation to different hosts and lifestyles but also signatures of common ancestry. *PLoS Genet.* **2012**, *8*, e1003088. [[CrossRef](#)] [[PubMed](#)]
22. Martin, F.; Kohler, A.; Murat, C.; Veneault-Fourrey, C.; Hibbett, D.S. Unearthing the roots of ectomycorrhizal symbioses. *Nat. Rev. Microbiol.* **2016**, *14*, 760–773. [[CrossRef](#)]
23. Nagy, L.G.; Riley, R.; Tritt, A.; Adam, C.; Daum, C.; Floudas, D.; Sun, H.; Yadav, J.S.; Pangilinan, J.; Larsson, K.-H.; et al. Comparative genomics of early-diverging mushroom-forming fungi provides insights into the origins of lignocellulose decay capabilities. *Mol. Biol. Evol.* **2016**, *33*, 959–970. [[CrossRef](#)] [[PubMed](#)]
24. Park, Y.J.; Jeong, Y.U.; Kong, W.S. Genome sequencing and carbohydrate-active enzyme (CAZyme) repertoire of the white rot fungus *Flammulina elastica*. *Int. J. Mol. Sci.* **2018**, *19*, 2379. [[CrossRef](#)] [[PubMed](#)]
25. Zhao, H.; Yan, B.; Mo, S.; Nie, S.; Li, Q.; Ou, Q.; Wu, B.; Jiang, G.; Tang, J.; Li, N.; et al. Carbohydrate metabolism genes dominant in a subtropical marine mangrove ecosystem revealed by metagenomics analysis. *J. Microbiol.* **2019**, *57*, 575–586. [[CrossRef](#)] [[PubMed](#)]
26. Arfi, Y.; Levasseur, A.; Record, E. Differential gene expression in *Pycnoporus coccineus* during interspecific mycelial interactions with different competitors. *Appl. Environ. Microbiol.* **2013**, *79*, 6626–6636. [[CrossRef](#)]
27. Saha, P.; Roy-Barman, S. The role of the global regulator of secondary metabolism laea in different fungi. *Curr. J. Appl. Sci. Technol.* **2018**, *31*, 1–5. [[CrossRef](#)]
28. Niemela, T.; Renvall, P.; Penttillä, R. Interactions of fungi at late stages of wood decomposition. *Ann. Bot. Fenn.* **1995**, *32*, 141–152.
29. Zhang, L.Y.; Wei, Y.L. Species diversity and distribution characters of wood-decaying fungi in Fenglin Nature Reserve. *Chin. J. Ecol.* **2016**, *35*, 2745–2751. [[CrossRef](#)]
30. Qin, J.; Horak, E.; Popa, F.; Rexer, K.H.; Yang, Z.L. Species diversity, distribution patterns, and substrate specificity of *Strobilurus*. *Mycologia* **2018**, *110*, 584–604. [[CrossRef](#)]
31. Wang, P.M.; Yang, Z.L. Two new taxa of the *Auriscalpium vulgare* species complex with substrate preferences. *Mycol. Prog.* **2019**, *18*, 641–652. [[CrossRef](#)]
32. Mayjonade, B.; Gouzy, J.; Donnadieu, C.; Pouilly, N.; Marande, W.; Callot, C.; Langlade, N.; Muñoz, S. Extraction of high-molecular-weight genomic DNA for long-read sequencing of single molecules. *Biotechniques* **2016**, *61*, 203–205. [[CrossRef](#)]
33. Zhu, N.; Huang, W.; Wu, D.; Chen, K.; He, Y. Quantitative visualization of pectin distribution maps of peach fruits. *Sci. Rep.* **2017**, *7*, 9275. [[CrossRef](#)] [[PubMed](#)]
34. Koren, S.; Walenz, B.P.; Berlin, K.; Miller, J.R.; Bergman, N.H.; Phillippy, A.M. Canu: Scalable and accurate long-read assembly via adaptive k-mer weighting and repeat separation. *Genome Res.* **2017**, *27*, 722–736. [[CrossRef](#)] [[PubMed](#)]
35. Lam, K.K.; Labutti, K.; Khalak, A.; Tse, D. FinisherSC: A repeat-aware tool for upgrading de novo assembly using long reads. *Bioinformatics* **2015**, *31*, 1–8. [[CrossRef](#)] [[PubMed](#)]
36. Liu, Y.C.; Jan, S.; Bertil, S. Musket: A multistage k-mer spectrum-based error corrector for Illumina sequence data. *Bioinformatics* **2013**, *29*, 308–315. [[CrossRef](#)]
37. Walker, B.J.; Abeel, T.; Shea, T.; Priest, M.; Abouelliel, A.; Sakthikumar, S.; Cuomo, C.; Zeng, Q.; Wortman, J.; Young, S.K.; et al. Pilon: An integrated tool for comprehensive microbial variant detection and genome assembly improvement. *PLoS ONE* **2014**, *9*, e112963. [[CrossRef](#)] [[PubMed](#)]
38. Huang, S.; Chen, Z.; Huang, G.; Yu, T.; Yang, P.; Li, J.; Fu, Y.; Yuan, S.; Chen, S.; Xu, A. HaploMerger: Reconstructing allelic relationships for polymorphic diploid genome assemblies. *Genome Res.* **2012**, *22*, 1581–1588. [[CrossRef](#)]
39. Huang, S.F.; Kang, M.J.; Xu, A.L. HaploMerger2: Rebuilding both haploid sub-assemblies from high-heterozygosity diploid genome assembly. *Bioinformatics* **2017**, *33*, 2577–2579. [[CrossRef](#)]
40. Sipos, G.; Prasanna, A.N.; Walter, M.C.; O'Connor, E.; Balint, B.; Krizsán, K.; Kiss, B.; Hess, J.; Varga, T.; Slot, J.; et al. Genome expansion and lineage-specific genetic innovations in the forest pathogenic fungi *Armillaria*. *Nat. Ecol. Evol.* **2017**, *1*, 1931–1941. [[CrossRef](#)]

41. Varga, T.; Krizsán, K.; Földi, C.; Dima, B.; Sánchez-García, M.; Sánchez-Ramírez, S.; Szöllösi, G.; Szarkándi, J.G.; Papp, V.; Albert, L.; et al. Megaphylogeny resolves global patterns of mushroom evolution. *Nat. Ecol. Evol.* **2019**, *3*, 668–678. [[CrossRef](#)]
42. Li, T.C.; Yu, L.Y.; Song, B.; Song, Y.; Li, L.; Lin, X.; Lin, S.J. Genome improvement and core gene set refinement of *Fugacium kawagutii*. *Microorganisms* **2020**, *8*, 102. [[CrossRef](#)] [[PubMed](#)]
43. Chen, L.; Gong, Y.; Cai, Y.; Liu, W.; Zhou, Y.; Xiao, Y.; Xu, Z.; Liu, Y.; Lei, X.; Wang, G.; et al. Genome sequence of the edible cultivated mushroom *Lentinula edodes* (shiitake) reveals insights into lignocellulose degradation. *PLoS ONE* **2016**, *11*, e0160336. [[CrossRef](#)]
44. Eastwood, D.C.; Floudas, D.; Binder, M.; Majcherczyk, A.; Schneider, P.; Aerts, A.; Asiegbu, F.O.; Baker, S.E.; Barry, K.; Bendiksby, M.; et al. The plant cell wall-decomposing machinery underlies the functional diversity of forest fungi. *Science* **2011**, *333*, 762–765. [[CrossRef](#)] [[PubMed](#)]
45. Floudas, D.; Binder, M.; Riley, R.; Barry, K.; Blanchette, R.A.; Henrissat, B.; Martínez, A.T.; Otilar, R.; Spatafora, J.W.; Yadav, J.S.; et al. The Paleozoic origin of enzymatic lignin decomposition reconstructed from 31 fungal genomes. *Science* **2012**, *336*, 1715–1719. [[CrossRef](#)]
46. Martinez, D.; Larrondo, L.; Putnam, N.; Gelpke, M.D.S.; Huang, K.; Chapman, J.; Helfenbein, K.G.; Ramaiya, P.; Detter, J.C.; Larimer, F.W.; et al. Genome sequence of the lignocellulose degrading fungus *Phanerochaete chrysosporium* strain RP78. *Nat. Biotechnol.* **2004**, *22*, 695–700. [[CrossRef](#)] [[PubMed](#)]
47. Ohm, R.A.; Riley, R.; Salamov, A.; Min, B.; Choi, I.G.; Grigoriev, I.V. Genomics of wood-degrading fungi. *Fungal Genet. Biol.* **2014**, *72*, 82–90. [[CrossRef](#)] [[PubMed](#)]
48. Olson, A.; Aerts, A.; Asiegbu, F.O.; Belbahri, L.; Bouzid, O.; Broberg, A.; Canbäck, B.; Coutinho, P.M.; Cullen, D.; Dalman, K.; et al. Insight into trade-off between wood decay and parasitism from the genome of a fungal forest pathogen. *New Phytol.* **2012**, *194*, 1001–1013. [[CrossRef](#)]
49. Suzuki, H.; MacDonald, J.; Syed, K.; Salamov, A.; Hori, C.; Aerts, A.; Henrissat, B.; Wiebenga, A.; Vankuyk, P.A.; Barry, K.; et al. Comparative genomics of the white-rot fungi, *Phanerochaete carnososa* and *P. chrysosporium*, to elucidate the genetic basis of the distinct wood types they colonize. *BMC Genom.* **2012**, *13*, 444. [[CrossRef](#)]
50. Oghenekaro, A.O.; Kovalchuk, A.; Raffaello, T.; Camarero, S.; Asiegbu, F.O. Genome sequencing of *Rigidoporus microporus* provides insights on genes important for wood decay, latex tolerance and interspecific fungal interactions. *Sci. Rep.* **2020**, *10*, 5250. [[CrossRef](#)]
51. Konno, K. Plant latex and other exudates as plant defense systems: Roles of various defense chemicals and proteins contained therein. *Phytochemistry* **2011**, *72*, 1510–1530. [[CrossRef](#)]
52. Keller, N.P.; Turner, G.; Bennett, J.W. Fungal secondary metabolism—From biochemistry to genomics. *Nat. Rev. Microbiol.* **2005**, *3*, 937–947. [[CrossRef](#)]
53. Devi, S.; Kiesewalter, H.T.; Kovács, R.; Frisvad, J.C.; Weber, T.; Larsen, T.O.; Kovács, T.; Ding, L. Depiction of secondary metabolites and antifungal activity of *Bacillus velezensis* DTU001. *Synth. Syst. Biotechnol.* **2019**, *4*, 142–149. [[CrossRef](#)] [[PubMed](#)]
54. Blin, K.; Medema, M.H.; Kazempour, D.; Fischbach, M.A.; Breitling, R.; Takano, E.; Weber, T. antiSMASH 2.0—a versatile platform for genome mining of secondary metabolite producers. *Nucleic Acids Res.* **2013**, *41*, W204–W212. [[CrossRef](#)]
55. Matys, V.; Fricke, E.; Geffers, R.; Gößling, E.; Haubrock, M.; Hehl, R.; Hornischer, K.; Karas, D.; Kel, A.E.; Kel-Margoulis, O.V.; et al. TRANSFAC1: Transcriptional regulation, from patterns to profiles. *Nucleic Acids Res.* **2003**, *31*, 374–378. [[CrossRef](#)] [[PubMed](#)]
56. Park, J.; Jang, S.; Kim, S.; Kong, S.; Choi, J.; Ahn, K.; Kim, J.; Lee, S.; Park, B.; Jung, K.; et al. FTFD: An informatics pipeline supporting phylogenomic analysis of fungal transcription factors. *Bioinformatics* **2008**, *24*, 1024–1025. [[CrossRef](#)] [[PubMed](#)]
57. Abascal, F.; Zardoya, R.; Posada, D. Prottest: Selection of best-fit models of protein evolution. *Bioinformatics* **2005**, *21*, 2104–2105. [[CrossRef](#)] [[PubMed](#)]
58. Katoh, K.; Standley, D.M. MAFFT multiple sequence alignment software version 7: Improvements in performance and usability. *Mol. Biol. Evol.* **2013**, *30*, 772–780. [[CrossRef](#)]
59. Stamatakis, A. RAxML version 8: A tool for phylogenetic analysis and post-analysis of large phylogenies. *Bioinformatics* **2014**, *30*, 1312–1313. [[CrossRef](#)]
60. Sanderson, M.J. r8s: Inferring absolute rates of molecular evolution and divergence times in the absence of a molecular clock. *Bioinformatics* **2003**, *19*, 301–302. [[CrossRef](#)]
61. Han, M.V.; Thomas, G.W.; Lugo-Martinez, J.; Hahn, M.W. Estimating gene gain and loss rates in the presence of error in genome assembly and annotation using CAFE 3. *Mol. Biol. Evol.* **2013**, *30*, 1987–1997. [[CrossRef](#)] [[PubMed](#)]
62. Johnston, S.R.; Boddy, L.; Weightman, A.J. Bacteria in decomposing wood and their interactions with wood-decay fungi. *FEMS Microbiol. Ecol.* **2016**, *92*, fiw179. [[CrossRef](#)] [[PubMed](#)]
63. Fukasawa, Y.; Matuoka, S. Communities of wood-inhabiting fungi in dead pine logs along a geographical gradient in Japan. *Fungal Ecol.* **2015**, *18*, 75–82. [[CrossRef](#)]
64. Friedemann, G.; Leshem, Y.; Kerem, L.; Shacham, B.; Bar-Massada, A.; McClain, K.M.; Bohrer, G.; Izhaki, I. Multidimensional differentiation in foraging resource use during breeding of two sympatric top predators. *Sci. Rep.* **2016**, *6*, 35031. [[CrossRef](#)]
65. Herzog, C.; Hartmann, M.; Frey, B.; Stierli, B.; Brunner, I. Microbial succession on decomposing root litter in a drought-prone scots pine forest. *ISME J.* **2019**, *13*, 2346–2362. [[CrossRef](#)]
66. Holmer, L.; Renvall, P.; Stenlid, J. Selective replacement between species of wood-rotting basidiomycetes, a laboratory study. *Mycol. Res.* **1997**, *101*, 714–720. [[CrossRef](#)]

67. Stokland, J.N.; Siitonen, J.; Jonsson, B.G. *Biodiversity in Dead Wood*; Cambridge University Press: Cambridge, UK, 2012.
68. Voříšková, J.; Baldrian, P. Fungal community on decomposing leaf litter undergoes rapid successional changes. *ISME J.* **2013**, *7*, 477–486. [[CrossRef](#)]
69. Floudas, D.; Bentzer, J.; Ahrén, D.; Johansson, T.; Persson, P.; Tunlid, A. Uncovering the hidden diversity of litter-decomposition mechanisms in mushroom-forming fungi. *ISME J.* **2020**, *14*, 1–14. [[CrossRef](#)]
70. Weng, C.H.; Peng, X.W.; Han, Y.J. Depolymerization and conversion of lignin to value-added bioproducts by microbial and enzymatic catalysis. *Biotechnol. Biofuels* **2021**, *14*, 84. [[CrossRef](#)] [[PubMed](#)]
71. Polo, C.C.; Pereira, L.; Mazzafera, P.; Flores-Borges, D.N.A.; Meneau, F. Correlations between lignin content and structural robustness in plants revealed by x-ray ptychography. *Sci. Rep.* **2020**, *10*, 6023. [[CrossRef](#)] [[PubMed](#)]
72. Adams, A.S.; Jordan, M.S.; Adams, S.M.; Suen, G.; Goodwin, L.A.; Davenport, K.W.; Currie, C.R.; Raffa, K.F. Cellulose-degrading bacteria associated with the invasive woodwasp *Sirex noctilio*. *ISME J.* **2011**, *5*, 1323–1331. [[CrossRef](#)]
73. Coates, D.; Rayner, A.D.M. Fungal population and community development in cut beech logs. III. Spatial dynamics, interactions and strategies. *New Phytol.* **1985**, *101*, 153–171. [[CrossRef](#)]
74. Abad, M.; Ansuategui, M.; Bermejo, P. Active antifungal substances from natural sources. *Arch. Org. Chem.* **2006**, *2007*, 116–145. [[CrossRef](#)]
75. Lima, G.; Arru, S.; de Curtis, F.; Arras, G. Influence of antagonist, host fruit and pathogen on the biological control of postharvest fungal diseases by yeasts. *J. Ind. Microbiol. Biotechnol.* **1999**, *23*, 223–229. [[CrossRef](#)]
76. Wilson, C.L.; Wisniewski, M.E.; Biles, C.L.; McLaughlin, R.; Chalutz, E.; Droby, S. Biological control of post-harvest diseases of fruits and vegetables: Alternatives to synthetic fungicides. *Crop Prot.* **1991**, *10*, 172–177. [[CrossRef](#)]
77. Alves, M.J.; Ferreira, I.C.F.R.; Martins, A.; Pintado, M. Antimicrobial activity of wild mushroom extracts against clinical isolates resistant to different antibiotics. *J. Appl. Microbiol.* **2012**, *113*, 466–475. [[CrossRef](#)]
78. Jonkers, W.; Rodriguez, E.A.E.; Lee, K.; Breakspear, A.; May, G.; Kistler, H.C. Metabolome and transcriptome of the interaction between *Ustilago maydis* and *Fusarium verticillioides* in vitro. *Appl. Environ. Microbiol.* **2012**, *78*, 3656–3667. [[CrossRef](#)]
79. Niego, A.G.; Raspé, O.; Thongklang, N.; Charoensup, R.; Lumyong, S.; Stadler, M.; Hyde, K.D. Taxonomy, diversity and cultivation of the Oudemansielloid/Xeruloid taxa *Hymenopellis*, *Mucidula*, *Oudemansiella*, and *Xerula* with respect to their bioactivities: A review. *J. Fungi* **2021**, *7*, 51. [[CrossRef](#)]
80. Fernandes, A.F.; Costa, L.; Sousa, J.R.; Zalocha, J.; Almeida, M.G. Biological activities of marine-derived actinomycetes: Testing the aqueous extracellular phase of *Streptomyces aculeolatus*. *Ann. Med.* **2019**, *51* (Suppl. 1), 44. [[CrossRef](#)]